

# WV303 – OSM ADTI Support: S11AC20034

---

## *Project Objective:*

To provide technical support to the US Office of Surface Mining and its associated state agencies and watershed organizations for the prevention and treatment of acid mine drainage through the following work tasks:

- Task1:           Treatment of High TDS Water**
- Task 2:           In Situ Field-Scale Treatment of Selenium-Bearing Spoil Units**
- Task 3:           Natural Attenuation of TDS in Mountaintop Mines**

## *Final Report*

December 20, 2012

Revised April 10, 2013

## *Submitted to:*

U.S. Department of Interior  
Office of Surface Mining

## *Submitted by:*

National Mine Land Reclamation Center  
West Virginia University  
PO Box 6064  
Morgantown, WV 26506-6064

# Table of Contents

<b>Table of Contents</b> .....	<b>2</b>
<b>List of Figures</b> .....	<b>3</b>
<b>List of Tables</b> .....	<b>4</b>
<b>Task 1: Treatment of High TDS Water</b> .....	<b>6</b>
Executive Summary .....	6
Introduction.....	6
Calculations .....	8
Materials and Methods .....	12
Equipment and supplies .....	12
Procedures .....	12
Results and Discussion .....	14
Previous Related Work .....	14
The Solubility of $K_2SO_4$ in Mixed Solvents.....	14
Environmental Samples.....	15
Project Scope of Work (Recent Work).....	21
Ethanolamine .....	21
Mine Drainage Treatment .....	22
Addition of Calcium .....	23
Conclusions.....	24
References.....	24
<b>Task 2: In Situ Field-Scale Treatment of Selenium-Bearing Spoil Units</b> .....	<b>26</b>
Executive Summary .....	26
Introduction.....	26
Materials and Methods .....	29
Experimental Array and Design .....	29
Material Composition.....	32
Water Sampling and Chemical Analysis.....	33
Results and Discussion .....	33
Time Series of Results.....	33
Statistical Analysis of Mean Concentrations.....	36
Se Fluxes .....	36

Sequestration Mechanism.....	39
Replication and Variability.....	39
Se Mobility Observations.....	40
Practical Implications.....	40
Conclusions.....	40
Acknowledgements .....	41
References.....	41
<b>Task 3: Natural Attenuation of TDS in Mountaintop Mines.....</b>	<b>43</b>
Executive Summary .....	43
Introduction.....	43
Materials and Methods .....	46
Results and Discussion .....	49
Effects on ion concentrations due to valley fill age.....	50
Effects on ion concentrations due to coal seams mined.....	60
Conclusions.....	66
References.....	67

## List of Figures

Figure 1: Ternary Diagram of the Solubility of $K_2SO_4$ in the Water/2-propanol System at 50°C (Thomsen, 2011) .....	10
Figure 2: Ternary Diagram of the Solubility of $K_2SO_4$ in the Water/Ammonia System at 60°C (Thomsen, 2011) .....	11
Figure 3: Solubility of $K_2SO_4$ in Water and Water-2-Propanol Mixtures.....	14
Figure 4: Plot of Theoretical Final TDS (mg/L) After Removal of $K_2SO_4$ by Ammonia Using Data of Koneczny, 1975 .....	15
Figure 5: Flowback Water Treatment with 2-propanol .....	16
Figure 6: Grams of $K_2SO_4$ Remaining (Red) and Fraction Removed (Blue) with Ethanolamine .....	21
Figure 7: Aluminum, Barium & Strontium Removal from Mine Drainage using 2-Propanol.....	22
Figure 8: Removal of Calcium and Sulfate from Mine Drainage Using 2-Propanol .....	23
Figure 9: Behavior of Calcium, Sulfate, Chloride and TDS upon Addition of $Ca^{+2}$ .....	24
Figure 10: Eh-pH Diagram for Soluble Se Species (blue) and Insoluble Solid Phases Containing Se (tan). Calculations are for 10-6M total Se and 10-3M total Fe at 25°C.....	27
Figure 11: Location Map of the Hobet Mine, Lincoln County, West Virginia .....	29
Figure 12: Plan View (a) and Cross Section View (b) of Cell Construction .....	31

Figure 13: Layout of Lysimeter Array, with Labels Showing ID Numbers of Individual Lysimeters .....	32
Figure 14: Raw Time Series of Se Concentrations Arranged by Treatment. Each plot shows replicates for different treatments. Treatment cells A= 0 in, B = 0.25 in, C = 2.25 in, D = 9 in and E = 18 in depth of Ferrihydrite.....	35
Figure 15: Time Series of Mean (X's) and Confidence Intervals (95%) for Se Concentrations of all Replicates within Treatment Classes (n=6 or less). Treatment cells A= 0 in, B = 0.25 in, C = 2.25 in, D = 9 in and E = 18 in depth of Ferrihydrite. ....	37
Figure 16: Time Series of Mean Se Flux (g/day) per Cell for each Treatment Class (n≤6). Treatment cells A= 0 in, B = 0.25 in, C = 2.25 in, D = 9 in and E = 18 in depth of Ferrihydrite. ....	38
Figure 17: Cumulative Se Fluxes for the Five Ferrihydrite Treatments: A = 0 in, B = 0.25 in, C = 2.25 in, D = 9 in and E = 18 in depths. ....	39
Figure 18: Acidity (mg/L) for Upper Freeport sites extrapolated to the year 2050. Horizontal dashed line represents the cutoff acidity to begin passive treatment (100 mg/L). CAD, cumulative average difference; LCL, lower confidence limit; UCL, upper confidence.....	45
Figure 19: Sulfate decline during 21 years after flooding of mine in the Pittsburgh coal seam (Demchak, 2005). The x-axis is years after mining completion .....	45
Figure 20: Average Se concentrations over time.....	46
Figure 21: Mine sites that were sampled during two sampling events.....	47
Figure 22: Major Ions Contributing to TDS .....	50
Figure 23: Sulfate concentrations as a function of valley fill age. ....	51
Figure 24: Sulfate concentrations as a function of valley fill age and flow regime. ....	51
Figure 25: HCO <sub>3</sub> concentrations as a function of valley fill age. ....	52
Figure 26: HCO <sub>3</sub> concentrations as a function of valley fill age and flow regime.....	53
Figure 27: Magnesium concentrations as a function of valley fill age.....	54
Figure 28: Magnesium concentrations as a function of valley fill age and flow regime.....	54
Figure 29: Calcium concentrations as a function of valley fill age.....	55
Figure 30: Calcium concentrations as a function of valley fill age and flow regime.....	56
Figure 31: Selenium concentrations as a function of valley fill age.....	57
Figure 32: Selenium concentrations as a function of valley fill age and flow regime.....	57
Figure 33: TDS concentrations as a function of valley fill age. ....	59
Figure 34: TDS concentrations as a function of valley fill age and flow regime. ....	60
Figure 35: Changes in sulfate concentrations over time as a function of coal seams mined.....	61
Figure 36: Changes in HCO <sub>3</sub> concentrations over time as a function of coal seams mined. ....	62
Figure 37: Changes in Mg concentrations over time as a function of coal seams mined.....	63
Figure 38: Changes in Ca concentrations over time as a function of coal seams mined. ....	64
Figure 39: Changes in Se concentrations over time as a function of coal seams mined. ....	65
Figure 40: Changes in TDS concentrations over time as a function of coal seams mined.....	66

## List of Tables

Table 1: Potassium Sulfate-Water-Ammonia System at 20°C .....	11
---	----

Table 2: Flowback Water Treatment using 2-propanol .....	16
Table 3: Molar Solubilities of some Compounds (Weast, 1972) .....	17
Table 4: Mine Drainage Treated with 2-Propanol and Ammonia .....	18
Table 5: Flowback Water Evaluated with Ammonia (Procedure 4, mean of 3 trials).....	19
Table 6: Flowback Water Evaluated with 2-propanol (Bottle Method, mean of 3 trials).....	20
Table 7: Flowback Water Evaluated with 2-propanol (Procedure 3, mean of 3 trials).....	20
Table 8: Major Ion Composition of the Organic Shale Interburden used in this Study .....	33
Table 9: Criteria Used for Valley Fill Selection .....	47
Table 10: Information taken at each Valley Fill Sample Point .....	48
Table 11: R2 Values for all Parameters and Comparisons .....	49

# **Task 1: Treatment of High TDS Water**

## **Executive Summary**

Coal mining and shale gas development are major contributors to total dissolved solids (TDS) issues in West Virginia. Coal mining in West Virginia normally generates high sulfate discharges. Neutralization of acid mine drainage (AMD) with lime also leads to high calcium in the water. Even though TDS concentrations are much lower in AMD than from wastewater created by shale gas development, it is a significant problem in West Virginia because of the prevalence of coal mining. Numerous technologies have been developed for TDS treatment over the years. However, one of the major shortcomings with available technologies is cost. Cost-effective treatment options for reducing TDS concentrations in discharges from coal mining operations and wastewater generated from shale gas development are needed.

Addition of co-solvents, usually organic compounds, to high salt solutions lowers the solubility of salts, precipitates them and renders the solution more usable. Recent research projects funded by the Department of Energy (DOE) and Office of Surface Mining (OSM) have studied the use of ethanolamine, 2-propanol and ammonia to demonstrate the degree to which co-solvents can modify the composition of solutions found in the energy industry, specifically coal mine drainage (OSM) and flowback water from horizontally drilled and hydraulically fractured gas wells (DOE).

Building upon previous studies to reduce high TDS concentrations from waste streams of prevalent industrial practices in West Virginia and the surrounding Appalachian area, this study focused on:

- the addition of co-solvents to precipitate solids out of an AMD discharge stream and shale gas well flowback water;
- recover the co-solvents once precipitation had occurred; and
- determine the reduction of TDS values found in the treated AMD discharge stream and the treated shale gas well flowback water.

The TDS values for flowback water were lowered from over 100,000 mg/L to less than 50,000 mg/L, deeming the water suitable for industry reuse based on active industry procedures. Coal mine drainages were less successfully treated directly, only insoluble sulfates were removed with organic solvents and alkaline earth hydroxides (not sulfate) were removed with ammonia.

The addition of extra calcium assisted in sulfate removal from coal mine water, which may allow more efficient reverse osmosis treatment. However, the co-solvent treatment cannot meet the proposed water quality standard of 500 mg/L for TDS that the State of West Virginia is considering.

## **Introduction**

TDS is an operational definition of the dissolved content in a water sample after all suspended matter has been removed. The value is derived by quantitatively determining the solids content of a solution by weighing the solid residue after evaporation of the solvent. The TDS value will be composed of the masses of various precipitated salts and neutral compounds. Volatile dissolved substances will be

evaporated and are not measured. Certain solid salts incorporate water that may not be removed by heating. The value is usually reported as milligrams of solid/liter of solution (mg/L).

Estimates of TDS can be acquired by measuring the conductivity of a solution or summing the concentrations of elements or compounds determined by solution analytical methods. The accuracy of conductivity measurements as an indicator suffers at high TDS concentrations due to ion pairing and summed analytical values require foreknowledge of the solution composition.

Coal mining typically discharges high sulfate drainage as a result of pyrite oxidation. The TDS is normally under 10,000 mg/L and the discharge limit is in the vicinity of 500 mg/L. Removal of TDS requires a general (non-specific) water treatment method. A traditional method is distillation, commonly used to prepare high quality laboratory water. Distillation boils off solvent and recovers it, but the general procedure is much like the one used for TDS determination, evaporation with a solid product.

Another general water treatment method is reverse osmosis. This technique uses a semi-permeable membrane between two chambers, one containing source water and the other containing product water. The membrane is permeable to water, not solutes. Pressure (energy) is applied to the source chamber, which reverses the normal osmotic flow, forcing water from the source side, through the membrane into the product side. Pure water is recovered and the source water is rendered more concentrated due to the loss of water through the membrane.

Reverse osmosis is often used to produce drinking water from seawater. Efficiencies, which are defined as percent product water recovered, can be up to 90%, which would create one liter of waste for every nine liters of product water. Seawater is composed of predominantly sodium and chloride ions.

Sodium chloride has a solubility of 35 g salt/100g water, or 350 g/kg water. Seawater has a salinity of 35 g/L and a density of 1.03 kg/L, which calculates to 34 g salt/kg water, 10% of saturation. Ninety percent (90%) efficiency (900 g water of the original 1,000 g passes the membrane) would concentrate the waste to 340 g/kg water, barely below the concentration at which sodium chloride would precipitate. Solid material that is introduced to or forms in reverse osmosis system clogs the membrane and stops water purification. Extra maintenance and cost are required when a membrane becomes clogged.

Coal mine drainage would have a fraction of the source water by-pass the treatment, since the target is 500 mg/L (0.5 g salt/kg water). A starting TDS of 6,000 mg/L, or 6 g/L with a density of 1 kg/dm<sup>3</sup>, contains 6 g salt/kg water. Neutralized coal mine drainage contains largely sulfate and calcium, if treated with calcium bases, otherwise sodium if sodium hydroxide (NaOH) were used. The solubility of gypsum is 2.4 g/kg water (Weast, 1972). Gypsum has a tendency to supersaturate; the source water salt content often exceeds gypsum solubility. Any residual calcium would precipitate gypsum in the reverse osmosis system as the volume of inlet water was decreased, precipitating solid gypsum and clogging the system.

This research began investigating the use of what is colloquially known as the salting out effect with the objective of removing sulfate precipitates from coal mine drainage so that membrane technologies can be used for further treatment. Previous work had concentrated on general aspects of ion removal from

coal mine drainage and shale gas development flowback water. Current work focuses more on coal mining issues.

The ultimate approach was to use a modification of the Solvay process, a commercial, industrial-process invented to produce sodium carbonate (soda ash) for salting out TDS. That process uses a sodium chloride solution (seawater), limestone ( $\text{CaCO}_3$ ) and ammonia as reagents with the recovery of most of the ammonia and isolation of solid soda ash. Ammonia functions both as a pH adjustment chemical and a solvent dielectric modifier.

Original study objectives were focused on the use of carbon dioxide ( $\text{CO}_2$ ) and ammonia gas to lower the concentration of divalent ions. However, environmental health and safety plans for the use and storage of these gases were not approved by West Virginia University in time to implement these research study objectives and therefore researchers adjusted the scope of the project to further evaluate the use of other solvent methods to reduce TDS concentrations.

Additional methods of dielectric reduction use miscible solvents to remove ions through solubility reduction in the mixed solvent system. The solvents are usually organic compounds (ammonia is an exception) such as alcohols and amines, which easily dissolve in water. Isopropanol (designated here as 2-propanol) was the solvent of choice in this work. Ethanolamine was also used.

### Calculations

The solubility of ionic compounds in water is influenced by the chemical potential of the solvent. An increase in ionic strength will, for example, increase solubility by promoting the formation of soluble ion pairs due to increased charge density. The usual expression for the chemical solubility of a binary solid is



with a solubility product constant,  $K_{sp}$ , defined by

$$K_{sp} = a_{\text{A}^+} a_{\text{B}^-} \quad (2)$$

where  $a_x$  is the activity of species X.

The activity of a solute is related to its concentration by the activity coefficient,  $\gamma$ ,

$$a_x = \gamma_x[X] \quad (3)$$

where  $\gamma_x$  depends on the ionic strength of a solution through, most simply, the Debye-Huckel equation (Castellan, 1964) and has a range from 0 to 1. The higher the ionic strength, for which TDS and conductivity are crude measures, the smaller  $\gamma$  becomes. Phenomenological, as the ionic strength (TDS) increases in an aqueous solution, the activity coefficient for each ion decreases and the dissolved concentration of ionic species must increase to maintain a constant activity (*Equation 3*). The

operational solubility, which is expressed in g solid/100g solvent, thus increases with ionic strength. Gypsum ( $\text{CaSO}_4 \bullet 2\text{H}_2\text{O}$ ) is more soluble in flowback water than in mine drainage than in distilled water.

The activity of an ion is a thermodynamic constant for a particular solvent and the solubility of a salt varies with solvent. The more polar (related to the dielectric constant) the solvent, the more capable it can dissociate the salt and dissolve the ions. The alcohol 2-propanol is less polar than water, thus gypsum is less soluble in 2-propanol than water. Mixtures of solvents have intermediate compound solubilities. Adding a miscible solvent, such as 2-propanol, to an aqueous salt solution will lower the dielectric constant of the solvent. This will lower the solubility of the salt and the salt will precipitate from the mixed water-alcohol solution. This process is known as salting out.

The behavior of solubility in mixed solvent systems can be illustrated by the water-2-propanol- potassium sulfate ( $\text{K}_2\text{SO}_4$ ) system, see **Figure 1**. The diagram was constructed by Thomsen (2011) with data from Konecny, et al. (1973, 1975). The left-side axis is the  $\text{K}_2\text{SO}_4$  axis, the right-side axis is water and the bottom axis is for 2-propanol. All axes are in units of percent weight; thus, the three components must add to 100 for any solution. The circles are experimental points. The line was calculated by Thomsen (2011) using his UNIQUAC computer model, which was developed to predict solubility in mixed solvent systems. Note that the line and first experimental point on the left ( $\text{K}_2\text{SO}_4$ ) axis lies at roughly 15. A purely aqueous solution of  $\text{K}_2\text{SO}_4$  is thus 15% salt and 85% water, a 15 g  $\text{K}_2\text{SO}_4$ /100 g solution. The water composition can be read by moving horizontally across from the point on the  $\text{K}_2\text{SO}_4$  to the water axis (right side, or by difference since this solution only contains water and salt). The solubility is 17.6 g  $\text{K}_2\text{SO}_4$ /100 g water ( $15 \times 100 / 85$ ) at 50°C. The density of the solution will be larger than 1 g/mL, so the TDS will be somewhat lower, but for comparative purposes the TDS was 150,000 mg/L.

The last (farthest right) experimental point on the **Figure 1** graph lies at 69% water. Following the line downward diagonally left gives the 2-propanol contribution, 29%. Reading the left hand axis by moving parallel to the water axis (diagonally upward) gives 2% (also determinable by difference) for the salt content (solubility). The solubility of  $\text{K}_2\text{SO}_4$  in that mixed solvent (29.6% 2-propanol and 70.4% water) is 2.04 g  $\text{K}_2\text{SO}_4$ /100 g solvent.

One hundred grams of a saturated solution of  $\text{K}_2\text{SO}_4$  in water will contain 15 g of  $\text{K}_2\text{SO}_4$ . Enough 2-propanol, 35.7 g, must be added to make the solvent composition 29.6% 2-propanol and 70.4% water. The final solvent mass will be 120.7 g, 35.7 g of which (29.6%) is 2-propanol mixed with the original 85 g of water. The solubility of  $\text{K}_2\text{SO}_4$  is 2 g/100 g in that solvent, thus 120.7 g of solvent will contain 2.4 g of  $\text{K}_2\text{SO}_4$ . The amount precipitated and to be separated is 12.6 g of  $\text{K}_2\text{SO}_4$  ( $15 - 2.4$ ).

Evaporation (and recovery) of 2-propanol will yield a solution containing 2.4 g of  $\text{K}_2\text{SO}_4$  in 85 g of water, or 28 g/kg water. Again assuming a 1 g/mL density, the solution has a TDS of 28,000 mg/L, an 81% reduction from the original 150,000 mg/L.

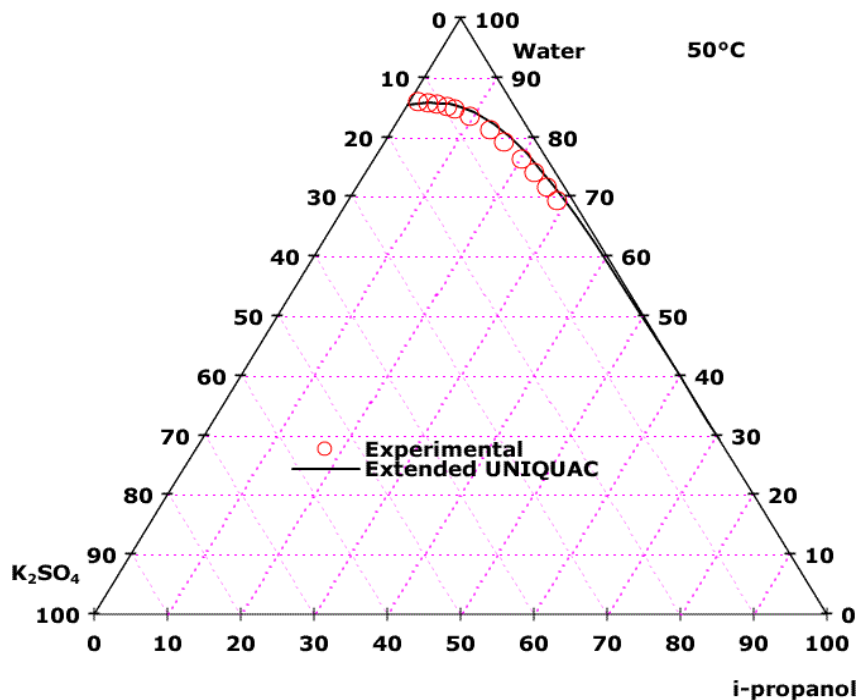


Figure 1: Ternary Diagram of the Solubility of  $K_2SO_4$  in the Water/2-propanol System at  $50^\circ C$  (Thomsen, 2011)

The  $K_2SO_4$ -water-ammonia ternary phase diagram, see **Figure 2**, reveals far less ammonia than 2-propanol, by weight, is needed to lower the  $K_2SO_4$  solubility. The plot as constructed by Thomsen is for  $60^\circ C$ , but Koneczny et al. (1975) have data for  $20^\circ C$ , which will be used here, see **Table 1**. The solution composition at  $20^\circ C$  as determined by Koneczny et al. (1975) was 10.01 g  $K_2SO_4$ /100 g solution. They reported the density as  $1.0818 \text{ g/cm}^3$ , so the TDS of the saturated  $K_2SO_4$  solution was 108,300 mg/L. At 15.1% ammonia, the  $K_2SO_4$  solubility was 0.98 g/100 g solution with a density of 0.9467 g/mL. The TDS of this solution is 9,280 mg/L. The solvent composition is 15.1 g of ammonia and 83.92 g water. Ammonia comprises 15.1% of the solution, but 15.25% of the solvent.

Calculating the removal process as for 2-propanol, 100 g of a saturated solution of  $K_2SO_4$  in water contains 10.01 g of  $K_2SO_4$  and 89.99 g of water. To make the solvent 15.25% ammonia [ $15.10 \text{ g NH}_3 / (15.10 \text{ g NH}_3 + 83.92 \text{ g H}_2\text{O})$ ] requires the addition of 16.2 g of  $NH_3$  (total solvent mass of 106.2 grams). The final solution will contain 1.05 g of  $K_2SO_4$ ; 8.96 g ( $10.01 - 1.05$ ) will precipitate. Removal of excess ammonia is easier than distilling off 2-propanol and once accomplished, the recovered 90 g of water will have 1.17 g  $K_2SO_4$ /100 g water. Assuming this density is 1 g/mL, the solution has a TDS of 11,700 mg/L, an 88.3% reduction in TDS.

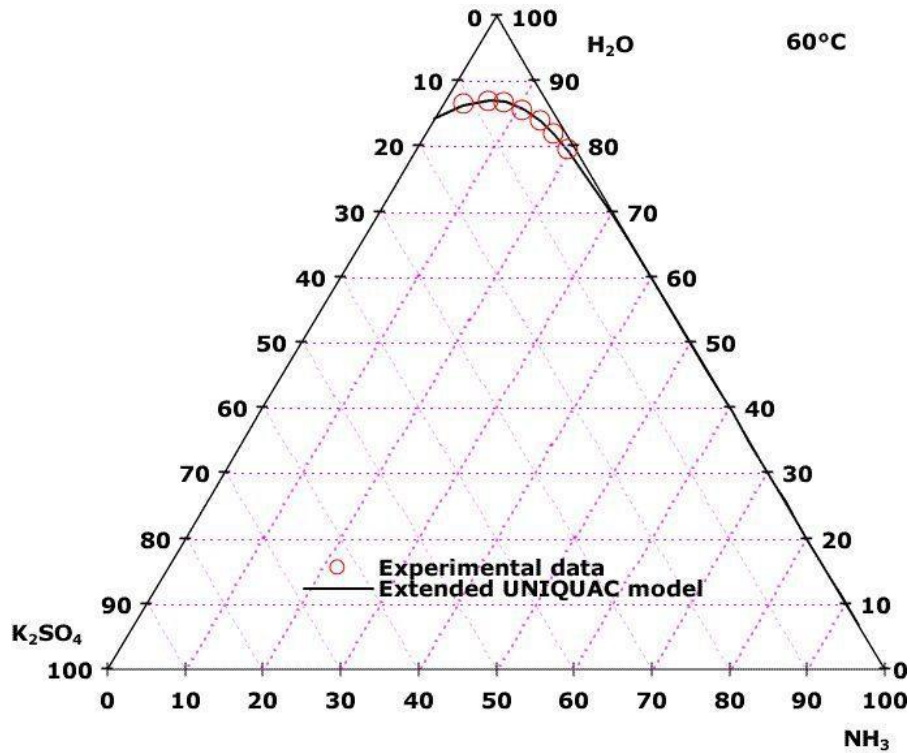


Figure 2: Ternary Diagram of the Solubility of  $K_2SO_4$  in the Water/Ammonia System at  $60^\circ C$  (Thomsen, 2011)

Table 1: Potassium Sulfate-Water-Ammonia System at  $20^\circ C$

Density g/cm <sup>3</sup>	Composition, weight %		
	$K_2SO_4$	$NH_3$	$H_2O$
1.0818	10.01	0.00	89.99
1.0353	6.56	2.82	90.52
1.0122	4.54	5.31	90.15
0.9832	2.75	8.41	88.84
0.9663	1.81	11.18	87.01
0.9467	0.98	15.10	83.92
0.9358	0.61	18.04	81.35
0.9216	0.38	20.89	78.73
0.9177	0.31	22.99	76.70
0.9096	0.22	25.18	74.60

Ammonia, and all gas solubility depends on Henry's Law (Castellan, 1964) which relates the amount of gas dissolved in a solvent as a function of pressure,

$$C_i = p_i/k_{Hi} \quad (4)$$

where  $C_i$  is the concentration of gas  $i$ ,  $p_i$  is the pressure of gas  $i$  and  $k_{Hi}$  is the unique, temperature dependent Henry's Law constant for gas  $i$ . Ammonia is a reactive gas, a weak base, which will react with water



The reactivity enhances the total solubility of ammonia over the Henry's Law value, making calculations of total dissolved ammonia more difficult. Addition of gaseous ammonia, as performed in the Solvay process, is far more complicated than simple liquid addition, but removal of gaseous ammonia afterwards is far easier than distillation.

Per gram co-solvent added, at least for potassium sulfate, ammonia is more efficient than 2-propanol, but ammonia solubility at atmospheric pressure maximizes at around 35 mass percent in water (Weast, 1972). Higher pressure application will dissolve more, as seen in *Equation 4*. 2-propanol is miscible with water in all proportions. It theoretically has greater utility to remove ions.

## Materials and Methods

### Equipment and supplies

250 mL beakers  
60 mL plastic bottles  
Deionized water  
100 mL graduated cylinder  
Stirring rod (or magnetic stirrer and bar)  
Weighing boat (or paper)  
Analytical balance  
Thermometer

### Procedures

#### Procedure 1: Beaker Solubility Method (aqueous solubility)

1. Use a graduated cylinder to add 100 mL of solvent to a 250 mL beaker.
2. Place a weighing boat (or piece of paper) on the balance and record its mass.
3. Add about 75 g of salt to the weighing boat. It does not have to be exactly 75 g, but record the mass of the weighing boat and salt to the nearest hundredth of a gram.
4. Slowly add about 5 g of the salt from the weighing boat to the beaker containing the 100 mL of solvent. Stir until all the salt is dissolved before adding any more salt.
5. Continue to gradually add salt to the water until no more will dissolve after you have stirred the solution for two minutes. The solution is now saturated.
6. Use a thermometer to record the final temperature of the saturated solution.
7. Weigh the weighing boat and the remaining salt and record.
8. Calculate the solubility.

Procedure 2: Bottle Solubility Method (mixed solvent solubility)

1. Weigh a dry 60 mL plastic bottle.
2. Place 10% more than the soluble amount of a dry salt (known mass) (KCl, K<sub>2</sub>SO<sub>4</sub>, etc.) in the bottle.
3. Weigh the bottle plus salt.
4. Add 50 mL of solvent.
5. Cap the bottle.
6. Weigh the bottle plus contents.
7. Shake/agitate (record time) until conductivity is constant.
8. Filter, dry and record recovered salt mass. Use minimal nonaqueous co-solvent for rinse.
9. Dry bottle and weigh.
10. Combine recovered salt mass and extra bottle mass.
11. Calculate solubility.

Procedure 3: Beaker Method for Environmental Samples

1. Acquire 1 liter or so of the environmental water sample.
2. If solids have not been removed, filter the water using a 0.45µm filter. Weigh the filter before and after filtering (air dry) to determine the solids content of the water.
3. Run a quick test first to see if salt is removed.
4. Weigh 100g of sample water into an appropriately sized beaker, 250 mL may be adequate.
5. Measure the conductivity of the solution.
6. Add 20g portions of co-solvent to the beaker. Measure the conductivity after each addition.
7. Upon observation of solid precipitation, add one additional portion of 20 g of co-solvent.
8. Recover the solid, dry and weigh. Save the liquid.
9. Evaporate off the co-solvent in a hood until 100 g of liquid remains (this will require evaporation, cooling and weighing, but the approximate volume should be obvious from the beaker).
10. Measure the conductivity of the remaining liquid.
11. Send the liquid for analysis. Analyze for the same ions determined in the original water.

Procedure 4: Evaporative Method for Environmental Samples

1. **PERFORM ALL AMMONIA OPERATIONS IN THE HOOD.**
2. Measure conductivity of water sample.
3. Add 50 mL samples in triplicate to weighed wide mouthed bottles.
4. Weigh sample plus bottle.
5. Gently evaporate to dryness, weigh when cooled.
6. Determine the solubility in 50 mL of 25% ammonia using the bottles method.
7. Scrape salt from bottle bottom during procedure if necessary.
8. Evaporate ammonia in hood until solution is nearly pH 8.
9. Determine conductivity of final solution.
10. Recover, dry and weigh any excess salt.
11. Have the solution(s) analyzed for appropriate ions.

## Results and Discussion

### Previous Related Work

Three classes of experiments were conducted using water, 2-propanol and a 25% aqueous ammonia solution. The solubilities of salts were determined in water and various solvent mixtures. Salting out of substances from solutions was measured and some environmental samples were treated using the two co-solvents.

### *The Solubility of $K_2SO_4$ in Mixed Solvents*

The solubility of  $K_2SO_4$  in water at 20°C using [Procedure 1](#) was determined to be 11.2 g/100 g water. The reference value (Weast, 1972) is 12 g/100 g at 25°C. Koneczny (1975) found the solubility to be 11.1 g/100 g at 20°C. [Procedure 4](#) was also tested by determining the solubility of  $K_2SO_4$  in water. A saturated solution of  $K_2SO_4$  was evaporated in triplicate and then dissolved. This second series yielded a solubility of 11.88 g  $K_2SO_4$ /100g water with a standard deviation of 0.015. This more complicated method was expected to be less accurate. The 6% larger solubility gave general credence to the method, but did not provide a superior solubility for  $K_2SO_4$ .

Experiments with  $K_2SO_4$ , see [Figure 3](#), showed 90% less solubility with 20% (w/w) 2-propanol than pure water. Determinations below 1 g  $K_2SO_4$ /100g were difficult to perform gravimetrically, thus higher amounts of 2-propanol were not used. The data conform to other experimental data as seen in [Figure 1](#). The initial TDS was 92,500 mg/L. At 20% 2-propanol, TDS was 13,300 mg/L after removing the 2-propanol.

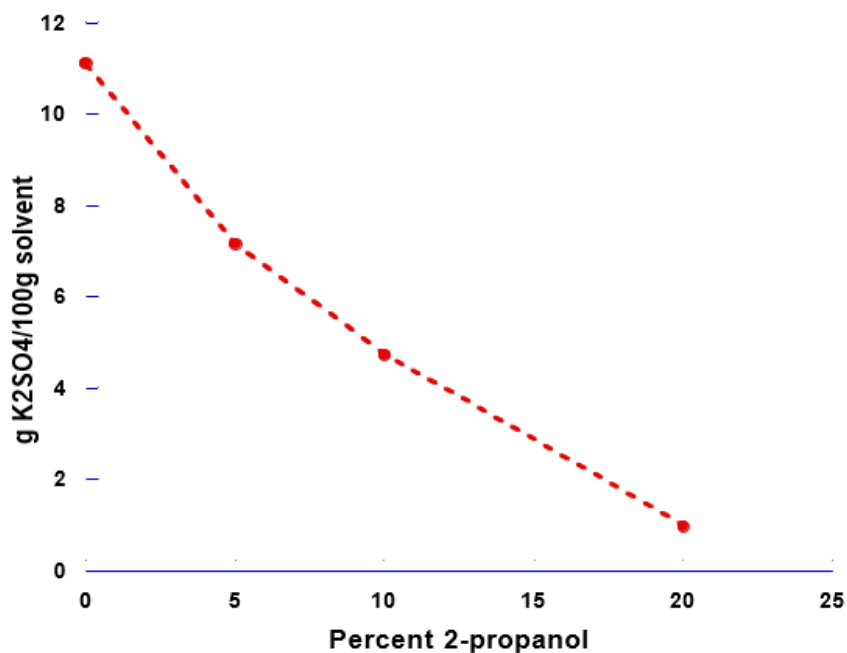


Figure 3: Solubility of  $K_2SO_4$  in Water and Water-2-Propanol Mixtures

The solubility of  $K_2SO_4$  in 25% ammonia solution yielded variable triplicate values with a mean of 0.43 g  $K_2SO_4$ /100 g solvent, and a standard deviation of 0.13. Koneczny (1975) found a value of 0.24 g/100 g for 25% ammonia. A plot of their data, see **Figure 4**, revealed that a 25% ammonia solution led to a TDS value of 2,400 mg/L. The direct conversion of our gravimetric results gives 4,300 mg/L. A sulfate determination of the recovered aqueous solution, when adjusted for stoichiometric potassium, yielded a TDS of 2,200 mg/L. For equal masses of additive, ammonia lowered the TDS more than 2-propanol, but more 2-propanol can conveniently be added to a solution, which will lower the TDS to levels below those achievable by ammonia.

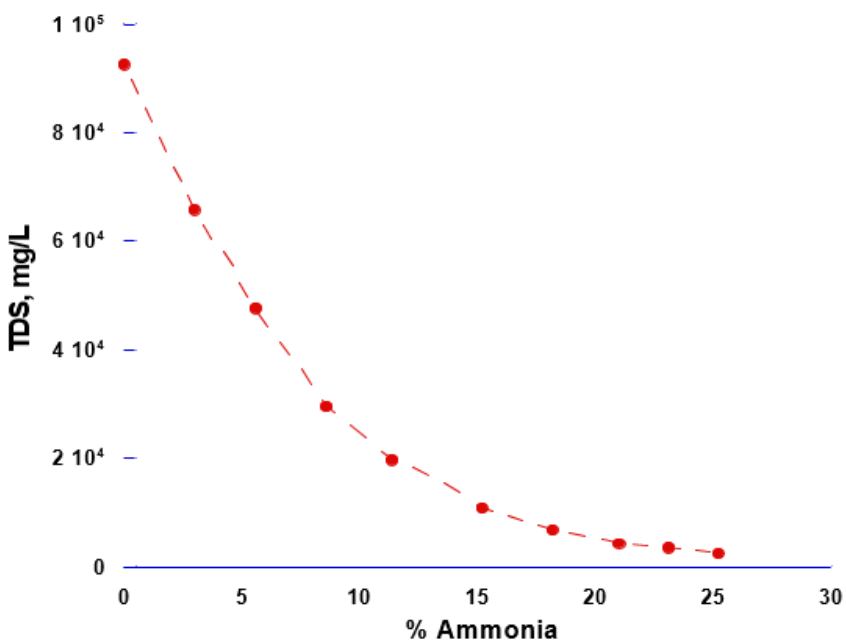


Figure 4: Plot of Theoretical Final TDS (mg/L) After Removal of  $K_2SO_4$  by Ammonia Using Data of Koneczny, 1975

### ***Environmental Samples***

#### **Flowback Water #1**

One hundred gram samples of shale gas well flowback water, see **Table 2**, were treated with 2-propanol using Procedure 3. The method is the obverse of the solubility experiments; 2-propanol was added to an existing solution. The behavior was tracked using conductivity. The added 2-propanol precipitated salt, which was isolated. The remaining 2-propanol was evaporated from the solution to yield an aqueous solution with a conductivity of 96 mS/cm, about half of the starting value of 198 mS/cm. The grams of 2-propanol added were halved to calculate the percentage of 2-propanol in the final solution.

The incremental reduction of TDS would be expected to decrease with low starting TDS due to the curvature of the TDS versus 2-propanol curve in **Figures 3 and 5**.

**Table 2: Flowback Water Treatment using 2-propanol**

	Original water mg/L	Treated water mg/L	Moles Removed	Percent Reduction
SO <sub>4</sub> <sup>-</sup>	48.5	<0.2	0.001	~100
Na	43,100	42,000	0.000	3
K	668	668	0.000	0
Cl <sup>-</sup>	107,000	105,600	0.039	1
Ca	21,200	423	0.519	98
Sr	2,970	<0.011	0.034	~100
Ba	1,280	<0.012	0.009	~100

SO<sub>4</sub> = sulfate, Na = sodium, K = potassium, Cl = chloride, Ca = calcium, Sr = strontium, Ba = barium

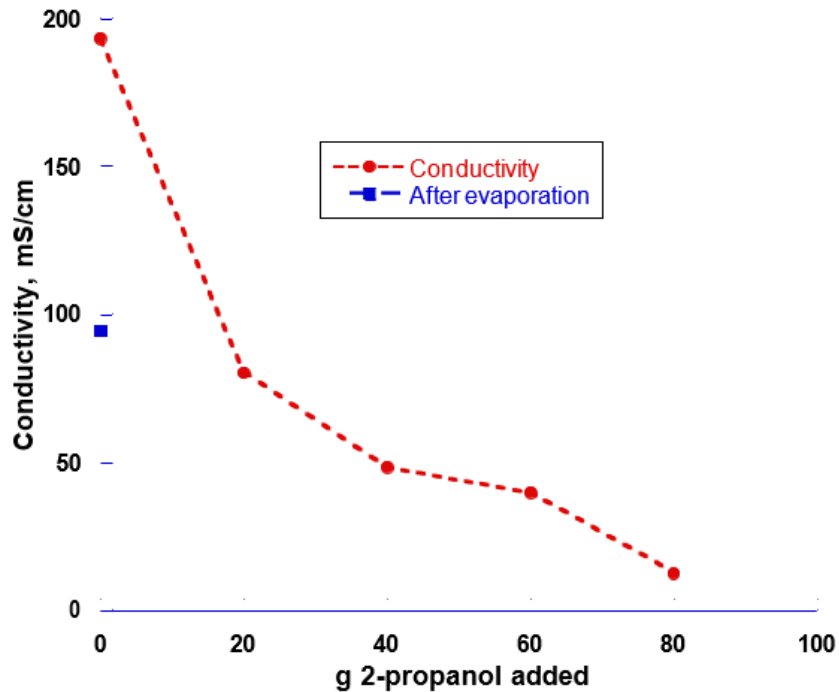


**Figure 5: Flowback Water Treatment with 2-propanol**

The resultant solutions were analyzed for the major ions as seen in **Table 2** showing significant reductions in the divalent cations calcium, strontium and barium, and anions sulfate and chloride.

Sulfate, sodium, potassium and chloride after sample treatment were determined by a different analytical laboratory than the alkaline earth elements. Potassium and sodium values increased after treatment according to the analyses. Accordingly, the K and Na values from that laboratory were adjusted to reflect no loss of potassium from the system. The reported K value, 1,004 mg/L, was set to 668 mg/L, the untreated value, and the ratio, 0.66, was applied to the sodium concentration.

The original TDS of the water was 189,000 mg/L. The sum of the original values in **Table 3** is 176,000 mg/L. Addition of magnesium and iron, which are not included in the table, raised the value to 178,000 mg/L, equating to 94% of the original value. The sum of the final concentrations is 144,000 mg/L, 76% of the original value. The conductivity of the final solution **Figure 5** was roughly half of the original solution. The discrepancy between the conductivity decrease and the calculated ion decrease is unknown pointing to the need of a more thorough examination not possible under the current study and time constraints. Possible explanations offered include an error in chloride analysis or the presence of some 2-propanol in the final solution that lowered the solvent dielectric constant.

**Table 3: Molar Solubilities of some Compounds (Weast, 1972)**

	Chloride, M	Hydroxide, M	Sulfate, M
Na	6.11	10.5	0.73
K	4.65	19.1	0.69
Ca	6.71	0.025	0.014
Sr	3.39	0.034	0.0006
Ba	1.80	0.178	0.00001

The reduction of alkaline earth ions is, to a small extent, due to alkaline sulfate precipitation; however, this possibility will only account for a small number of moles. **Table 3** shows the hydroxides of the alkaline earth ions to be very insoluble and, given the small chloride decrease, probably account for much of the precipitation. **Table 3** also contains approximate solubilities and shows that the chlorides are very soluble. The solids were not characterized. The calculated TDS of 144,000 mg/L for the treated flowback water is not sufficient to allow re-use of the water. The addition of more 2-propanol may treat the water to below 50,000 mg/L; but, additional testing was not attempted due to this study focusing more on treatment of TDS from mine water discharge than shale gas well flowback water.

#### Mine Drainage

Procedure 4 was developed in order to maximize the percentage of ammonia available as a co-solvent. The method along with Procedure 3 using 2-propanol was applied to mine water. The mine water, described in **Table 4**, had a reduction of calcium from 798 mg/L to 156 mg/L using 2-propanol.

Strontium (Sr) decreased, but barium (Ba) showed no change, largely due to limit of detection differences between laboratories. Sulfate decreased and comparison of the millimolar losses in column 4 of **Table 4** shows that calcium and sulfate loss are of the same magnitude, indicating possible gypsum loss.

**Table 4: Mine Drainage Treated with 2-Propanol and Ammonia**

	Original mg/L	2-propanol mg/L Left	2-propanol mmoles Removed	25 % Ammonia mg/L Left
Ca	798	156	16.05	25.2
Sr	6.68	0.11	0.075	
Ba	0.005	0.006	0	
SO <sub>4</sub> <sup>=</sup>	6,250	5,200	10.94	6,960

Ammonia removed more calcium and no sulfate (Sr and Ba were not measured). The calcium removal is due to calcium hydroxide precipitation, not gypsum, referring to **Table 4**. Ammonia is a base and supplies hydroxide to the system. The TDS of the original mine drainage was 2,840 mg/L which is smaller than the measured sulfate concentration of 6,250 mg/L. This may be caused by the conversion factor used when converting conductivity measurements to TDS concentrations. The water does not have enough calcium to remove the entire sulfate loading when the 2-propanol is added. The sulfate may be removable by addition of calcium, as lime, followed by 2-propanol induced precipitation. As applied, neither ammonia nor 2-propanol can reduce the TDS of the mine water to 500 mg/L directly. Ammonia has no intrinsic capability to remove sulfate at such low levels, but 2-propanol can non-specifically remove it. The large difference in TDS and sulfate is likely caused by disconnect in data manipulation for these two parameters. TDS is converted from conductivity which uses a conversion factor with a wide range, 0.54 – 0.96. Sulfate data comes directly from laboratory analyses.

#### Flowback Water #2

A second flowback water sample was tested with 25% ammonia and 2-propanol using Procedures 3 and 4. The flowback water had an initial pH of 6.6. After re-dissolving the salt in ammonia solution, then driving off much of the ammonia, the pH was measured at 8.2. The solution contained 680 mg/L ammonia nitrogen, 826 mg/L ammonia, indicating over 96% removal of ammonia from the solution. The conductivity increased from 13.9 mS/cm<sup>2</sup> to 15 mS/cm<sup>2</sup>, an increase of 7.9% and attributed to ammonium.

**Table 5** shows ion concentrations decreased substantially for the alkaline earth elements (magnesium, calcium, strontium and barium), by one third for sulfate, and marginally for potassium and chloride. The TDS for the original flowback water was 9,760 mg/L, which is rather low to expect substantial removal

by solubility decrease. The solubility of pure  $K_2SO_4$  in 25% ammonia is 0.22g/100g solvent, roughly 2.2 g/L, far in excess of the 43 mg/L seen here.

**Table 5: Flowback Water Evaluated with Ammonia (Procedure 4, mean of 3 trials)**

	Original water mg/L	Treated water mg/L	Percent reduction %
Ca	698	10.3	98.5
Sr	51	7.5	86
Ba	14	0.063	99.5
Mg	60	<0.5	>99
SO <sub>4</sub> <sup>-</sup>	19	11.9	37
K	43	37.3	13
Cl	4,600	4,160	10

The removal of alkaline earth ions is largely through precipitation of their hydroxides at the high pH of the initial ammonia solution. That solution was filtered, then the ammonia driven off for the final pH of 8.2. The hydroxide solubilities are Ba>Sr>Ca>Mg. The sulfate solubilities are Mg>Ca>Sr>Ba. The removal order in ammonia is Ba>Mg>Ca>Sr, with barium out of order. The very low barium value is likely due to some barium sulfate precipitation, making it less concentrated than the strontium.

Procedure 4 using 2-propanol is more indicative of dielectric constant lowering. See **Table 6**. Barium and strontium, the least soluble sulfates, were decreased, while magnesium and calcium were barely removed. The sulfate decrease indicates removal by barium and strontium, although a mass balance does not provide enough sulfates to account for all the strontium. The chloride decrease cannot be balanced by the measured cations. Sodium (unmeasured) is likely the cation associated with chloride. The flowback water contained 2,060 mg/L sodium, but its removal was not measured in the treated samples. The conductivity decreased to 0.67 mS/cm<sup>2</sup>, a 95% decrease. Roughly half the salt isolated from the flowback water dissolved in the 2-propanol, whereas 84% dissolved in the 25% ammonia solvent.

Table 6: Flowback Water Evaluated with 2-propanol (Bottle Method, mean of 3 trials)

	Original water mg/L	Treated water mg/L	Percent reduction %
Ca	698	629	0.9
Sr	51	14.8	71
Ba	14	0.27	98
Mg	60	56	6.8
SO <sub>4</sub> <sup>=</sup>	19	5.54	71
K	43	4.9	89
Cl	4,600	1,117	76

The less difficult Procedure 3 was conducted using 2-propanol. Two hundred grams of 2-propanol were added to 100 g of the flowback water. The 2-propanol was evaporated and water recovered. Very little solid was generated and with the exception of barium, very little change in concentration for the ions is seen as detailed in **Table 7**. The conductivity of the resultant solutions averaged 14 mS/cm<sup>2</sup>. Procedure 3 has been shown to successfully remove salts from flowback waters with high concentrations of dissolved solids as seen in **Table 2**; but, this water was too dilute. The intent was to lower TDS concentrations of flowback water to 50,000 mg/L; however, this water had an initial TDS value of 10,000 mg/L TDS, characteristic of early-stage flowback. Barium removal was consistent in all cases. The change in solvent polarity lowered the solubility, which is small even in water, and removed barium as the sulfate. Other ions were not removed. Some ions showed a negative removal. The final volume in all three treatments was less than the starting volume, hence some ions showed higher concentrations.

Table 7: Flowback Water Evaluated with 2-propanol (Procedure 3, mean of 3 trials)

	Original water mg/L	Treated water mg/L	Percent reduction %
Ca	698	801	-15
Sr	51	54.5	-7
Ba	14	1	93
Mg	60	69	-14
SO <sub>4</sub> <sup>=</sup>	19	16.5	13
K	43	41.5	3
Cl	4,600	4,240	8

## Project Scope of Work (Recent Work)

### Ethanolamine

The solubility of  $K_2SO_4$  in water with the addition of ethanolamine ( $H_2NCH_2CH_2OH$ , 2-amino ethanol) was determined, as seen in **Figure 6**. Ethanolamine has intermediate properties between 2-propanol and ammonia (it is a weak base). Ethanolamine boils at  $16.5^\circ C$ , in contrast to  $82.5^\circ C$  for 2-propanol, so its removal would be more cost effective. A sample consisting of 100.06 g of deionized water and 11.13 g of  $K_2SO_4$  had successive amounts of ethanolamine added.

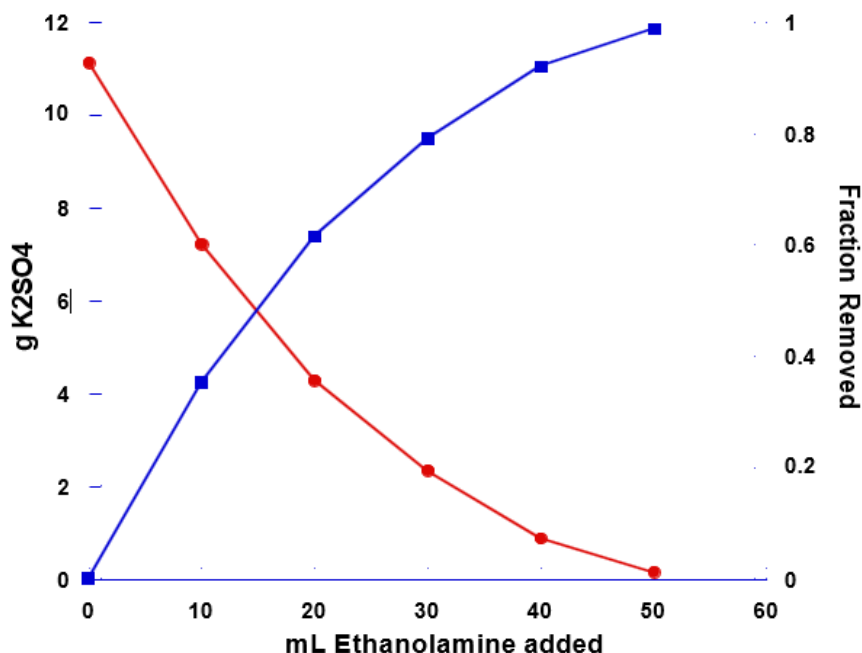


Figure 6: Grams of  $K_2SO_4$  Remaining (Red) and Fraction Removed (Blue) with Ethanolamine

The precipitated salt was isolated after each addition. The density of ethanolamine is  $1.018 \text{ g/mL}$ . The solution at 40 mL added ethanolamine consisted of 0.88 g of  $K_2SO_4$ , 100.06 g water and 40.72 g of ethanolamine. When normalized to 100%, the solution was 0.06%  $K_2SO_4$ : 70.6%  $H_2O$ : 28.7% ethanolamine. The solvent was 71% water and 29% ethanolamine. Removal of  $K_2SO_4$  was superior to ammonia, referring back to **Table 1**, largely because more ethanolamine can be added to solution. At 20 mL (20.36 g) added ethanolamine, 4.28 g of  $K_2SO_4$  remains in solution. The normalized values at 20 mL added are 3.4%  $K_2SO_4$ : 80.2%  $H_2O$ : 16.3% ethanolamine. Interpolation of **Table 1** shows superior removal by ammonia on a mass basis in this case.

**Figure 3** shows the solubility of  $K_2SO_4$  in water: 2-propanol mixtures. A solvent that was 20% 2-propanol contained 6.74 g of the salt. The solvent consisted of 80 g water and 20 g 2-propanol. The percent normalized values were 6.3%  $K_2SO_4$ : 74.9%  $H_2O$ : 18.7% 2-propanol. Removal by isopropanol may be a

little worse than with ethanolamine, but the comparison is not exact. Removal is of the same magnitude. Ethanolamine, as noted, can be removed from its mixture with water more easily, at the cost of less energy, than 2-propanol. This factor makes it the superior choice.

**Mine Drainage Treatment**

Mine drainage was treated with 2-propanol. More ions were monitored than seen in **Table 4**. Fifty mL samples of mine water were treated with 25, 50 and 100 mL of 2-propanol, refer to **Figures 7 and 8**. Ions not shown (Fe, Cl, Na, Mg) were not affected. Barium was present at a very low level, near the detection limit, and any barium in the system is likely removed by formation of BaSO<sub>4</sub>. Aluminum, strontium, calcium and sulfate all decreased with added isopropanol. Most of the decrease in species concentration occurred with the addition of the smallest amount of 2-propanol. Smaller removals occurred with addition of more co-solvent. As noted above, calcium (and strontium) removes as much sulfate as possible. Calcium is reduced by 800 mg/L (20 mM). If calcium were precipitated by sulfate, that would involve loss of 20 mM of sulfate or 1,892 mg/L. The sulfate concentration decreased 2,585 mg/L. No attempt was made to account for the other 600 mg/L loss of sulfate.

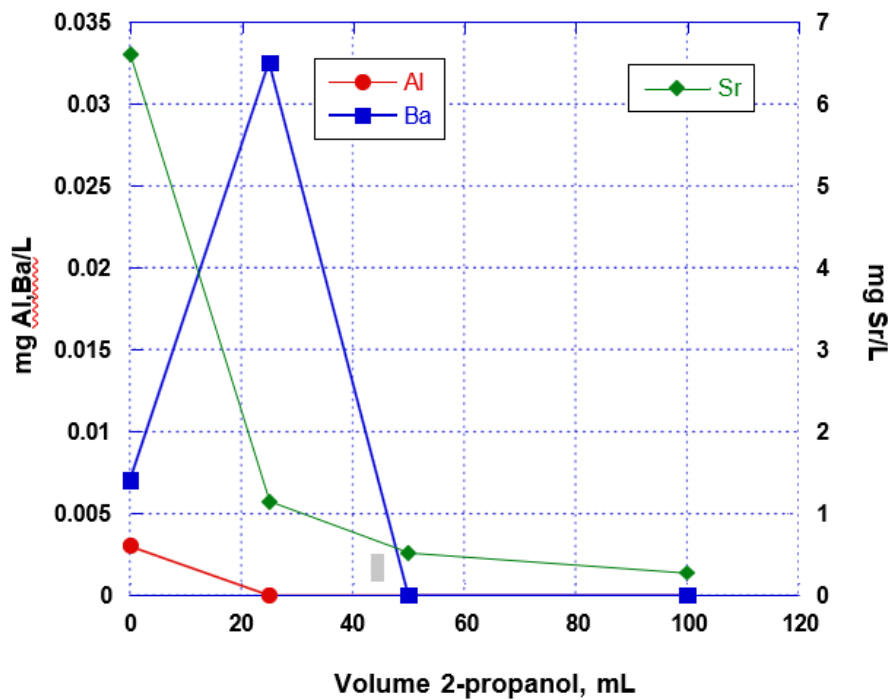


Figure 7: Aluminum, Barium & Strontium Removal from Mine Drainage using 2-Propanol

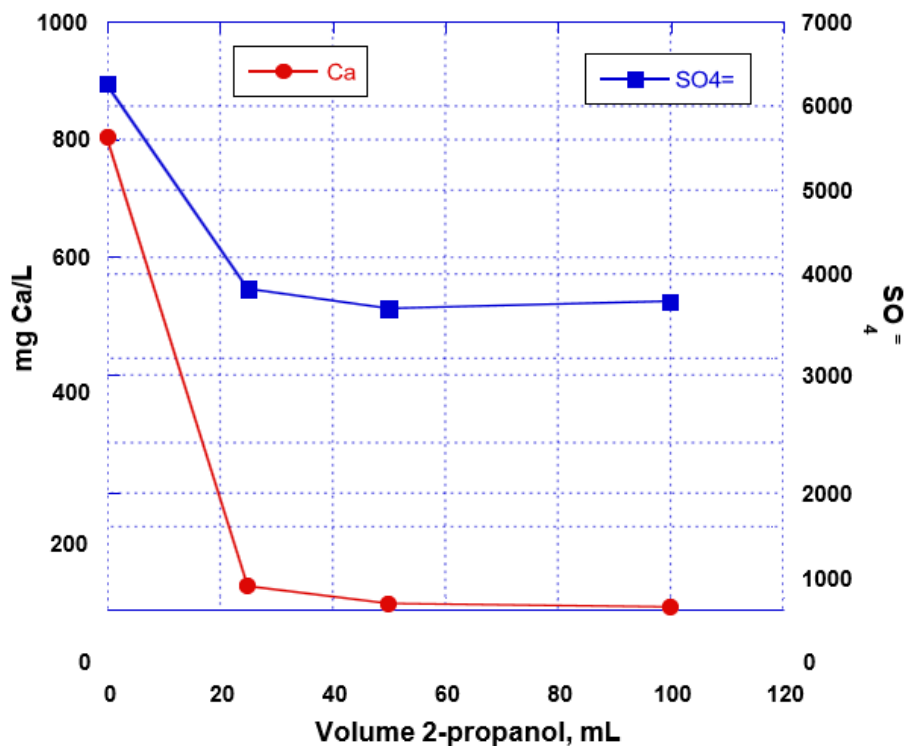


Figure 8: Removal of Calcium and Sulfate from Mine Drainage Using 2-Propanol

### ***Addition of Calcium***

The removal of sulfate from mine drainage will lower the total dissolved solids and make the water more amenable to general methods of TDS reduction, such as reverse osmosis, without membrane clogging. Coal mine drainage quality is not dramatically improved by co-solvent methods, as shown in **Table 4**. Strontium and barium, and calcium less efficiently, are removed (as sulfates) by organic co-solvents, but the sulfate is removed to a much less extent because its concentration greatly exceeds the amount of calcium and other divalent cations. Ammonia removes calcium very efficiently as the hydroxide, but removes none of the sulfate.

Experiments were conducted that involved adding excess calcium to mine drainage samples in order to more fully precipitate the sulfate, see **Figure 9**. A 0.1M solution of  $\text{CaCl}_2$  was prepared and added to 50 mL of the mine drainage used for **Figures 7 and 8**. The added calcium allows the sulfate to be removed. The sulfate drops from 6,250 mg/L to 200 mg/L after addition of 50 mL of calcium solution. The TDS does not change much; sulfate is being replaced by chloride in the TDS. Calcium is low (400 mg/L) in spite of the added calcium, which is largely removed as gypsum. Upon adding 100 mL of calcium solution, the calcium and chloride concentrations and the TDS increase sharply since no further sulfate is available for reaction.

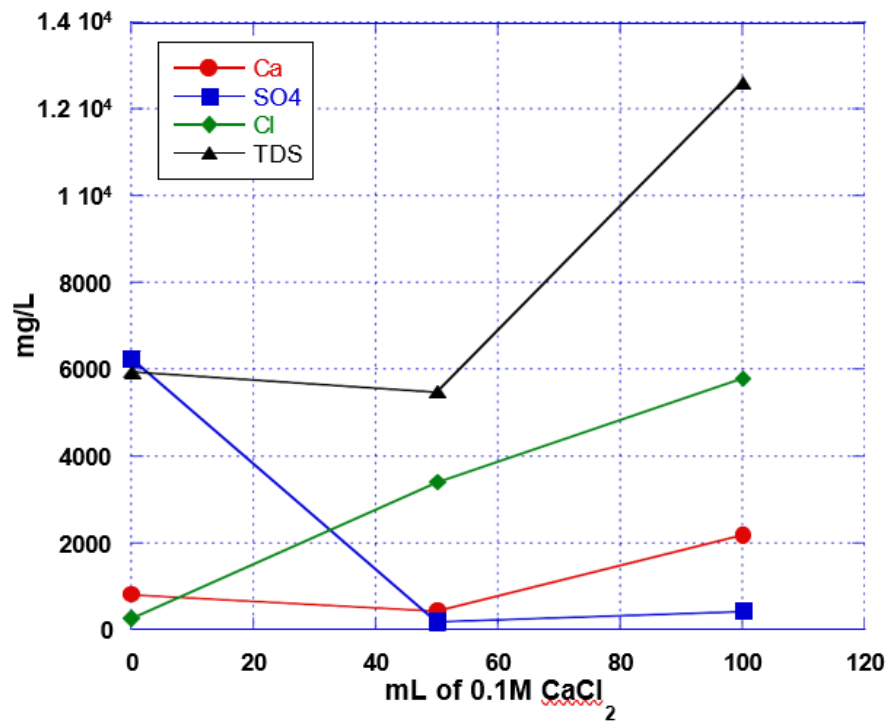


Figure 9: Behavior of Calcium, Sulfate, Chloride and TDS upon Addition of Ca<sup>+2</sup>

## Conclusions

Salt (e.g., K<sub>2</sub>SO<sub>4</sub>) solubility can be lowered in mixed solvent system such as water and 2-propanol, water and ammonia, and this principle can be used to treat TDS from mine drainage and flowback water. The laboratory experiment showed that addition of co-solvents can remove ions from solution, most commonly sulfate and alkaline earth ions. For flowback water, calcium, strontium and barium can be effectively removed. Sulfate can be partially removed, but monovalent ion (sodium, potassium and chloride) removal is minimal. For mine drainage water, 2-propanol has potential to lower TDS if sulfate and calcium are major components of the drainage. The addition of extra calcium can assist in sulfate removal from coal mine water. Removal of sulfate will also improve the utility of reverse osmosis as a water treatment option to lower TDS to 500 mg/L with additional treatment such as reverse osmosis. Lowering the potential for precipitation of relatively insoluble compounds, which is essentially the outcome of co-solvent addition, should improve the performance and lower the cost (through membrane lifetime increase and higher efficiency) of reverse osmosis.

## References

Castellan, G.W. (1964), *Physical Chemistry*, Addison-Wesley, Reading, MA.

Koneczny, H., Lango, D, and Lango, M., (1973) Badania Układu KCl-NH<sub>3</sub>-H<sub>2</sub>O, *Chemia Stoswana*, **17**, 115-125.

Koneczny, H., Lango, D, and Lango, M., (1975) Badania Układu K<sub>2</sub>SO<sub>4</sub>-NH<sub>3</sub>-H<sub>2</sub>O, *Chemia Stoswana*, **19**, 27-36.

Thomsen, K. (2011) <http://www.phasediagram.dk/mixeds/>

Weast, R.C. (1972), *Handbook of Chemistry and Physics*, 53<sup>rd</sup> Ed., The Chemical Rubber Co., Cleveland, OH.

## **Task 2: In Situ Field-Scale Treatment of Selenium-Bearing Spoil Units**

### **Executive Summary**

Thirty lysimeters were installed at the Hobet Mine located in southeast West Virginia in Spring 2010 to test for transport rate of selenium in mine-run interburden as well as selenium removal by adsorption to layered ferric oxyhydroxide (ferrihydrite). Each 16 x 24 foot cell contained about 61 tons (4 to 6 foot thickness) of Stockton/Coalburg seam interburden, overlaying various thicknesses (0.25, 2.25, 9, and 18 inches, plus a zero-amendment control cell) of fine-grained ferrihydrite from a limestone-treated acid mine drainage (AMD) wetland. The mass of ferrihydrite was 0 to 2.2% weight percent of the spoil. The control and each amendment were replicated 6 times, for estimation of uncertainty in reproducibility of results. Rainfall was collected on and infiltrated through these cells to create a leachate that drained to individual central collection tanks. Sampling was performed 46 times at approximate 2 week intervals from 2010-2012. Basal ferrihydrite layers in the three highest amendment categories successfully removed up to 76.9% selenium (in comparison to the unamended piles) from leachate by an adsorption mechanism. Results were somewhat variable for replicates. The higher amendment concentrations were demonstrably more effective, while the very-thin ferrihydrite-treated piles showed no significant reduction from unamended piles. Reproducibility of replicates was in general acceptable for both amended and unamended lysimeters. Work now focuses on continuing the time series to assess long-term persistence of selenium fluxes, examine the ultimate capacity of the ferrihydrite beds, and to geochemically model the adsorption and transport processes.

A paper based on the work conducted under this task has been accepted for publication in the *Journal of Environmental Quality*. A copy of the article will be provided to OSM once final edits have been completed.

### **Introduction**

It has been widely observed that selenium (Se) fate and transport in coal overburden materials may be influenced by mining and reclamation operations (Dreher and Finkelman, 1992). Predicting the fate and transport of Se mobilized from within coal mine spoil requires an understanding of the amount, form, and redox state of the element present; the rate and mechanism(s) of solubility; and the tendency for adsorption within the spoil mass post-dissolution (Naftz and Rice, 1989). Se concentrations in southern West Virginia coal overburden lithologies range from 0.84 mg/kg in sandstone to 4.10 mg/kg in organic shale, with high Se concentrations co-varying with high sulfur levels (Vesper et al., 2008). The proportion of mobile Se was estimated by Roy (2005) using extreme sequential extraction methods to accelerate and maximize its dissolution rate. She estimated that roughly 50% of total Se in overburden is non-extractable while another 25% is bound in non-mobile organic form. Most of the remaining 25% potentially mobile Se was inferred in this study to occur either within sulfide minerals or as adsorbed ions. Similar estimates were obtained for mobile Se (35% and 38% of total Se) using extraction by sonication of two similar organic shales from southern West Virginia (Pumure et al. 2010). All these sequential extraction estimates should be considered upper limits on field Se solubility, obtained under more intense weathering conditions than found in nature. Emerson et al. (2009) determined the more-reactive fine fraction (<2 mm) as 34% for southern West Virginia coal mine spoil that had been exposed

to weathering for one to two years. Diehl et al. (2005) determined Se in pyrite in southern Appalachian coals by a variety of micro-analytical techniques. Whole-coal values for Se ranged from 25 to 247 mg/kg, while 670 mg/kg Se was found in pyrite alone, roughly 2 to 20% of the Se in the coal. This Se percentage for pyrite correlates well with the fraction found in sulfides by Roy (2005) (8 % in the pyrite fraction of coal, 13% in shale).

Thus the most likely primary solid-phase occurrence of Se is in sulfide minerals, either in pyrite or ferroselite ( $\text{FeSe}_2$ ), its Se-bearing analog. An Eh-pH diagram for Se species (**Figure 10**) shows areas of thermodynamic stability for elemental zero-valent Se ( $\text{Se}^0$ ) as well as more reduced iron selenides. The pourbaix diagram is meant to be illustrative. The specific stability fields would change in according to mineralogy and Eh/pH relationships within different spoil types. The principal soluble species are selenate and selenite, obtained by oxidation of these source solid phases. The oxidation of selenite to selenate, the more mobile aqueous species, requires higher oxidation potential than for sulfide dissolution. Vesper et al. (2008) showed that the proportion of selenate to selenite only gradually increased downstream of source coal mines. Selenite is generally the most abundant Se species reported in various power plant ash materials (Huggins et al., 2007), although Hyun et al. (2006) also found significant selenate. Zhang and Sparks (1992) observed that while both aqueous phases are amenable to adsorption on crystalline iron oxides, selenite is less rapidly adsorbed, but more tightly held, than selenate.

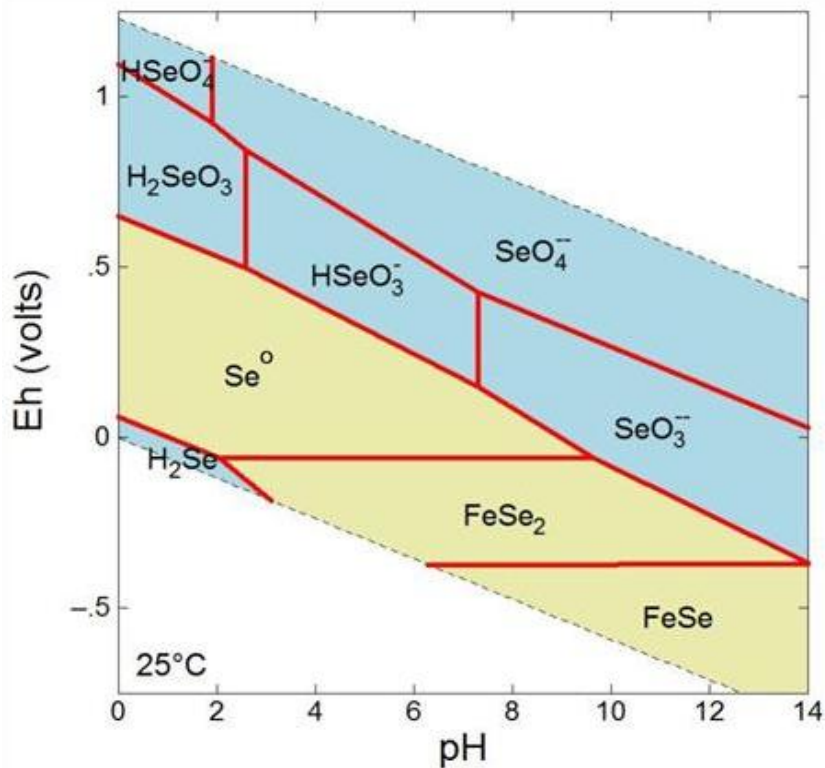


Figure 10: Eh-pH Diagram for Soluble Se Species (blue) and Insoluble Solid Phases Containing Se (tan). Calculations are for 10-6M total Se and 10-3M total Fe at 25°C.

Ferrihydrite or similar iron oxyhydroxides, a common neutralization product of treated metal-rich mine drainage, is thought to be a principal adsorbent for sequestering Se dissolved from coal waste rock. Ferrihydrite removed 95% of selenite at pH 4 and 80% at pH 9 (Merrill et al., 1985). Su and Suarez (2001) reached similar conclusions for amorphous iron oxide and its more crystalline phase goethite ( $\alpha$ -FeOOH), although the amorphous phase showed less capacity for adsorption. Zhang and Sparks (1990) examined the reaction rates of selenate and selenite sorption on goethite and concluded that selenite formed an inner sphere complex, whereas selenate formed a less strongly-bound, but more rapidly formed, outer sphere complex. Ziemkiewicz et al. (2011) added ferrihydrite to Se-bearing mine spoil in batch reactors and found that roughly 70% of available Se was immobilized by adsorption compared to untreated controls.

While laboratory leaching results provide insight into weathering and leaching mechanisms, the more salient issue to the mining and regulatory sectors is the concentration of total Se that will discharge from operating mines over time. Se discharge dynamics under field conditions are poorly understood, largely due to the slow nature of field weathering processes, the low concentrations of Se involved, and the relatively short time for which Se has been monitored in mined areas. Se was not considered a pollutant in Appalachian coal mining until about 2003, after which several large surface mines were required to sample and report Se discharged via their regulated water outlets. Ziemkiewicz and Lovett (2012) developed a chronosequence relating the age of various coal mine spoil units to selenium concentrations in outlets monitored over an eight year period. They reported that selenium concentrations ranged from 25 - 100  $\mu\text{g/L}$  in young spoil to < 5  $\mu\text{g/L}$  in spoil that was more than about 25 years old indicating a relatively rapid selenium removal rate. Nonetheless, there has been insufficient opportunity to develop a regional sense for how long or at what concentrations mobilizable Se will discharge from mined spoil materials via leachate. Se concentrations vary substantially among different lithologies. The Se concentration in a given discharge will thus integrate drainage from selenium-rich sources like organic shales, diluted by water from selenium-poor rock units and surface runoff. So it is pivotal to find techniques to isolate selenium-rich rock units and then minimize the leaching of selenium from them.

Another complicating factor at field scales of leaching is the heterogeneity of composition of spoil materials and how this might influence its Se leaching characteristics. Large-scale surface coal mining in the dissected Appalachian plateau involves multiple coal seams, overburden and interburden sequences as well as a mixture of sedimentary lithologies. However, spoil created and emplaced by mining methods is generally well-mixed within individual sequences. Roughly half the overburden/interburden at a modern mine is moved by cast-blasting and the other half by dragline or shovel/truck haulage. Excavated spoil is generally replaced by backfill along an advancing sloped face from 10 to 50 m long. Such handling methods result in a high degree of overburden blending. Weathering begins immediately after disaggregation of the rock by mining. Spoil age refers to the length of time since a rock unit was mined. While each lithology within a sequence will behave differently with regard to Se mobility, spoil units are highly mixed composites of the overburden lithologies. Segregation of the selenium-rich rock units opens the possibility of treatment directed at specific lithologies to strategically limit Se release.

Finally, the well-known heterogeneous nature of fluid flow systems that develop in coal-mine spoil adds another aspect of variability. Double-porosity characteristics, flow through conduit-like networks, and linear-flow characteristics have been observed and documented in the Appalachians (Maher and Donovan, 1997; Hawkins, 2004). In field trials, the vagaries of different fluid flowpath networks may cause differences in leaching intensity to be observed between spoil piles. In summary, for reasons of inherent variability in spoil composition and in the resulting fluid flow systems through spoil piles, field- scale experiments must incorporate adequate replication to verify the significance of chemical fluxes observed at the discharge.

The purpose of this study is to provide some initial estimates of selenium mobility in the presence of varying amounts of adsorbent materials, as well as to test for the uniformity of spoil-pile chemistry and hydrology at field leaching scale, rather than laboratory scale. This particular investigation focuses strictly on Se leaching behavior over a period of three years of initial exposure of fresh waste-rock spoil to infiltration and weathering. The study area is the Hobet Mine, Lincoln County, WV (**Figure 11**). This is an area where surface mining has been practiced for about 30 years and is ongoing.

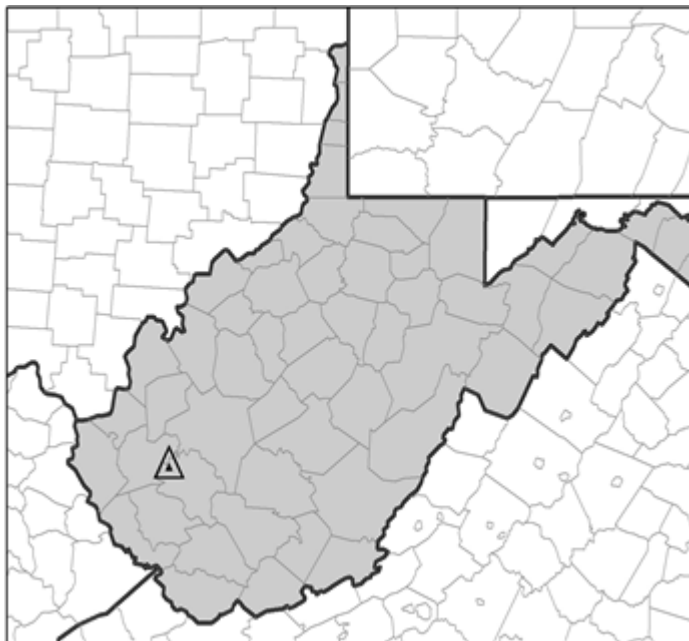


**Figure 11: Location Map of the Hobet Mine, Lincoln County, West Virginia**

## **Materials and Methods**

### **Experimental Array and Design**

Thirty pan-type lysimeters of large size (16 x 24 foot; **Figure 12**) were constructed at the Hobet Mine in Spring 2010. The individual lysimeter cells were constructed in a continuous array (**Figure 13**) of two

rows of 15 cells each, separated by a 6-ft high plywood inner wall. The outer walls of both rows were 4 feet high; thus the side partitions between cells and the soil surface were sloped gently from inner to outer walls. The cells were lined along the base and sides with 4-mil polyethylene and filled with (from bottom to top) a thin ferrihydrite layer, shaly waste rock, and a ca. 1-foot topsoil layer of weathered brown sandstone (**Figure 11**). The base of the liner was gently sloped roughly parallel to the soil surface, inducing basal gravity drainage from the inner to outer wall of each cell (**Figure 12**). Treatments consisted of five ferrihydrite layers, varying in thickness from 0.25 inches to 18 inches, covered with the same amount of shaly waste rock and top soil with six replicates. Treatments and replications were completely randomized. Each randomized experimental unit was assigned a number from 1 to 30, with a suffix to identify material composition. Additionally, the slope of the lysimeter array in each row (cells 1 to 15 and 16 to 30) was about 1:20 from north to south, allowing gravity drainage of collected lysimeter leachate in that direction. Each cell contained a two-inch perforated-PVC lateral underdrain in the ferrihydrite layer, located along the downgradient side wall and sloped from inner to outer wall, where it was collected in a non-perforated 0.75 inch ABS pipe bundled in an array with pipes from all 15 cells in that row. Within each lysimeter, drainage pipe was bedded and overlain with #57 limestone. While the original design called for a bed of gravel along the entire base of each lysimeter, this was not implemented. Each pipe bundle directed flow continuously under gravity to an array of thirty 330-gallon polyethylene tanks, each receiving water from a single lysimeter (**Figure 13**). Precipitation onto the soil of each cell either infiltrated or ran off onto native soil around the array, allowing no runoff between or onto adjacent lysimeters. Perennial grass/legume cover on the surface of each cell induced some evapotranspiration. The difference between surface infiltration and evapotranspiration constitutes recharge into each cell, which seeps deeply into the overburden soils and collects on the bottom liner, flowing into the diversion pipes and each cell's respective sample tank. The sample tank for each cell thus contained a time-integrated volume of leachate fluids collected during multiple recharge events between sampling dates.

The average depth of all material in each cell was from 4.0 to 6.0 feet (**Figure 12**), with an average volume of 766.8 ft<sup>3</sup>. The total mass was approximately 61.0 tons for an average field-moisture bulk density of 2.53 g/cm<sup>3</sup>.

The lysimeters were laid out according to **Figure 13**. The principal investigator, Ziemkiewicz, and his subcontractor were present during construction. However, when a crew from the company's subcontractor labeled the plots some time later, they apparently read the plot diagram as though looking at the plots from the north rather than from the access point at the south. In other words, it was thought that lysimeter 1 was closest to the collection tank gallery. However, this was not the case resulting in labeling rotated 180 degrees such that lysimeter 1, for example, was mislabeled lysimeter 30 and lysimeter 30 was mislabeled lysimeter 1. The leachate collection tanks were similarly mislabeled. The treatments were randomized so the lysimeter designations (1-30) had no systematic relationship to the treatments. Mislabeled thus had the effect of divorcing the results from the treatments. Therefore, results reported over the first two years appeared to have a great deal of error and no treatment effect. Various explanations were given by WVU's contractor including terminating the project. In May 2012, the principal investigator visited the treatment study site and discovered the mislabeling. The labeling

of the lysimeters and leachate collection tanks was corrected and the data identification of sampling results also corrected to accurately capture the true treatment of each lysimeter. Upon review of the data correlated with the correct lysimeter cell, strong treatment effects were noted and are therefore reported herein.

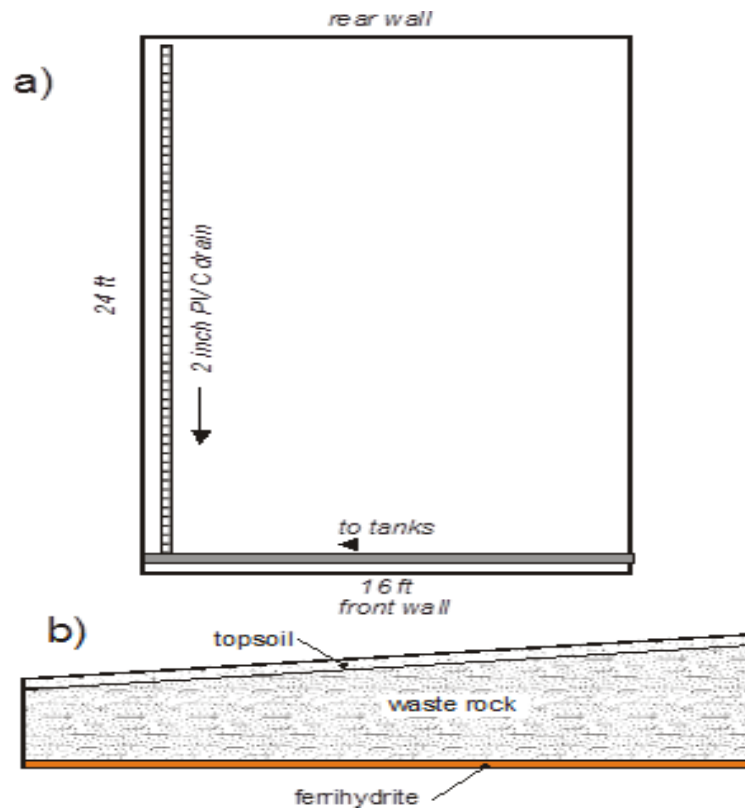


Figure 12: Plan View (a) and Cross Section View (b) of Cell Construction

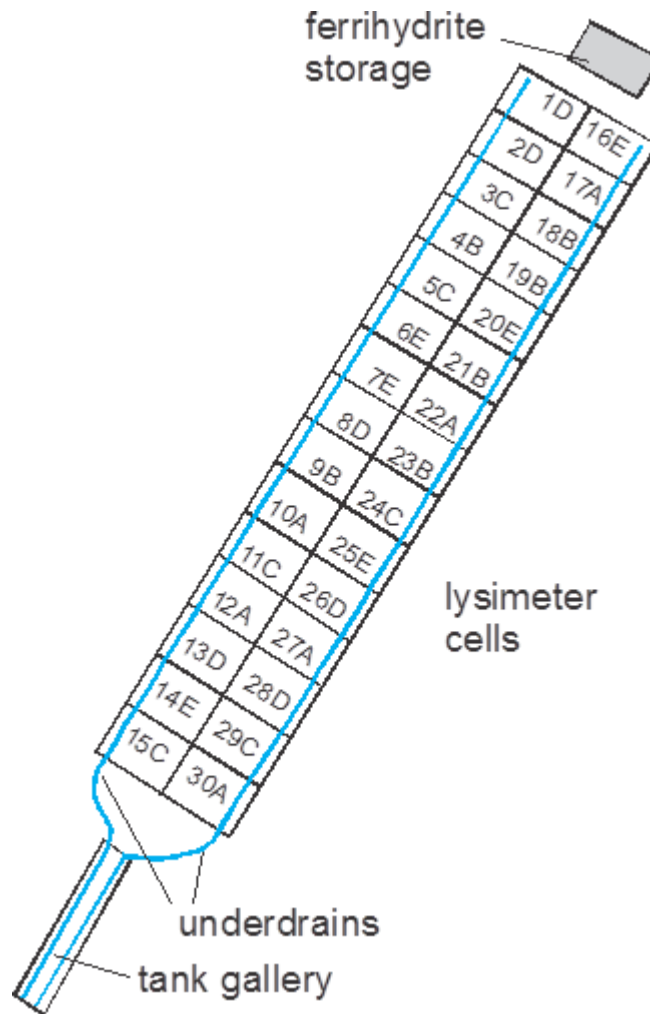


Figure 13: Layout of Lysimeter Array, with Labels Showing ID Numbers of Individual Lysimeters

### Material Composition

Each cell contained approximately the same volume of waste rock, measured by counting excavator buckets during construction, but various amounts of ferrihydrite, measured as a uniform thickness at the base of the spoil, immediately over the liner. The waste rock was sampled during construction in three 5-gallon pails and analyzed chemically. The waste rock was freshly-mined organic shale that forms the interval between the Stockton and Coalburg coal seams. The rock was homogeneous in appearance, stockpiled in a single day of mining for use in this project. **Table 8** summarizes the composition of the interburden.

**Table 8: Major Ion Composition of the Organic Shale Interburden used in this Study**

Analyte (all total)	Method	MDL	PQL	Result	Units
Ca	SW6010C	5	25	382	mg/kg
Fe	SW6010C	5	25	4210	mg/kg
Mg	SW6010C	1	12.5	497	mg/kg
Mn	SW6010C	0.2	2.5	17.1	mg/kg
S	SW6010C	20	50	2170	mg/kg
Se	SW6010C	1	5	3.24	mg/kg
% Moisture	SM2540G	NA	0.01	12	mg/kg

The ferrihydrite was obtained from a large wetland near Pittsburgh, Pennsylvania, in which limestone-treated AMD sludge had settled over a period of 30+ years, producing a reaction product with negligible aluminum and of high uniformity. The layer thickness and weight/weight ratio of ferrihydrite to spoil for each treatment (A-E) are as follows.

- A – No ferrihydrite (6 lysimeters)
- B – 0.25 inch (0.2%) inch ferrihydrite (6 lysimeters)
- C – 2.25 inch (1.5%) inch ferrihydrite (6 lysimeters)
- D – 9 inch (6%) ferrihydrite (6 lysimeters)
- E – 18 inch (12%) ferrihydrite (6 lysimeters)

Therefore, the array includes 6 identical replicates of each treatment, to allow for assessment of sampling error and uncertainty in material variation/hydrologic conditions.

**Water Sampling and Chemical Analysis**

Sampling was performed biweekly beginning on May 14, 2010 through June 1, 2012. On each date, the fluid volumes in the collection tanks were measured, samples collected, and each tank drained. Field pH, temperature, and conductivity were measured and the filtered samples were immediately taken to the laboratory (REI Consultants, Beaver, WV) and analyzed for total Se, SO<sub>4</sub>, alkalinity to pH 4.5 endpoint, acidity, Fe, Al, Ca, Mg, Mn, Na, and Cl. The water in the tanks and collection drains was found to be frozen on 12/10/2010 (week 30). Sampling resumed on 4/8/2011 (week 48). There were several sampling events in Fall 2010 when some tanks were dry due to lack of infiltration and no samples could be collected. Also, when tanks and lines thawed in April to May 2011, there were some tanks/lines which took longer to re-establish flow than others. Therefore, the number of replicates for each treatment was usually, but not always, six. During exceptionally dry periods, most if not all replications were dry. Thus on some dates, as few as one sample per replicate set was collected, affecting precision estimates.

**Results and Discussion**

**Time Series of Results**

**Figure 14** shows time series of selenium for the five treatments. Each plot shows a set of 6 different replicate time series for total selenium concentration in one treatment class, with each replicate

obtained from a different lysimeter. The ferrihydrite addition decreases from top (zero ferrihydrite) to bottom (maximum ferrihydrite, 18 inches). This plot shows general coherence in concentration between individual replicate sets, although there is evident variance within treatments as well. In particular, the first and second replicates in all treatments but especially C, D, and E – the circles and triangle symbols in these plots – were notably and in some cases markedly higher than the other replicates in their sets. It is conceivable that this could represent systematic natural variability in the refuse; all these cells are in the same portion of the array, from cells 1-12 (**Figure 13**) and were the first installed. It may also be that there was some difference in the installation of these lysimeters, either in the composition of the refuse used for those cells, in the compaction method, or in the technique used for leveling the PVC drain line within the ferrihydrite layer. Excepting this variability, there is generally minor variance between replicates within treatments, and variance within treatments seems greatest at times of highest Se concentration, which occurred in spring of both 2010 and 2011. That is, the coefficient of variation of Se concentrations tended to be uniform.

There was a gap in sampling between late November 2010 and early April 2011, caused by freezing of line drainage between the lysimeters and the tanks. During winter 2011-12, no freeze-up occurred. As a result, in addition to the Winter 2010-11 data gap, several sampling events in Fall 2010 and Spring 2011 had fewer than six replicates per treatment, as some drain lines thawed before others. Also, there were some periods in 2010 when some lysimeters produced no water during dry conditions.

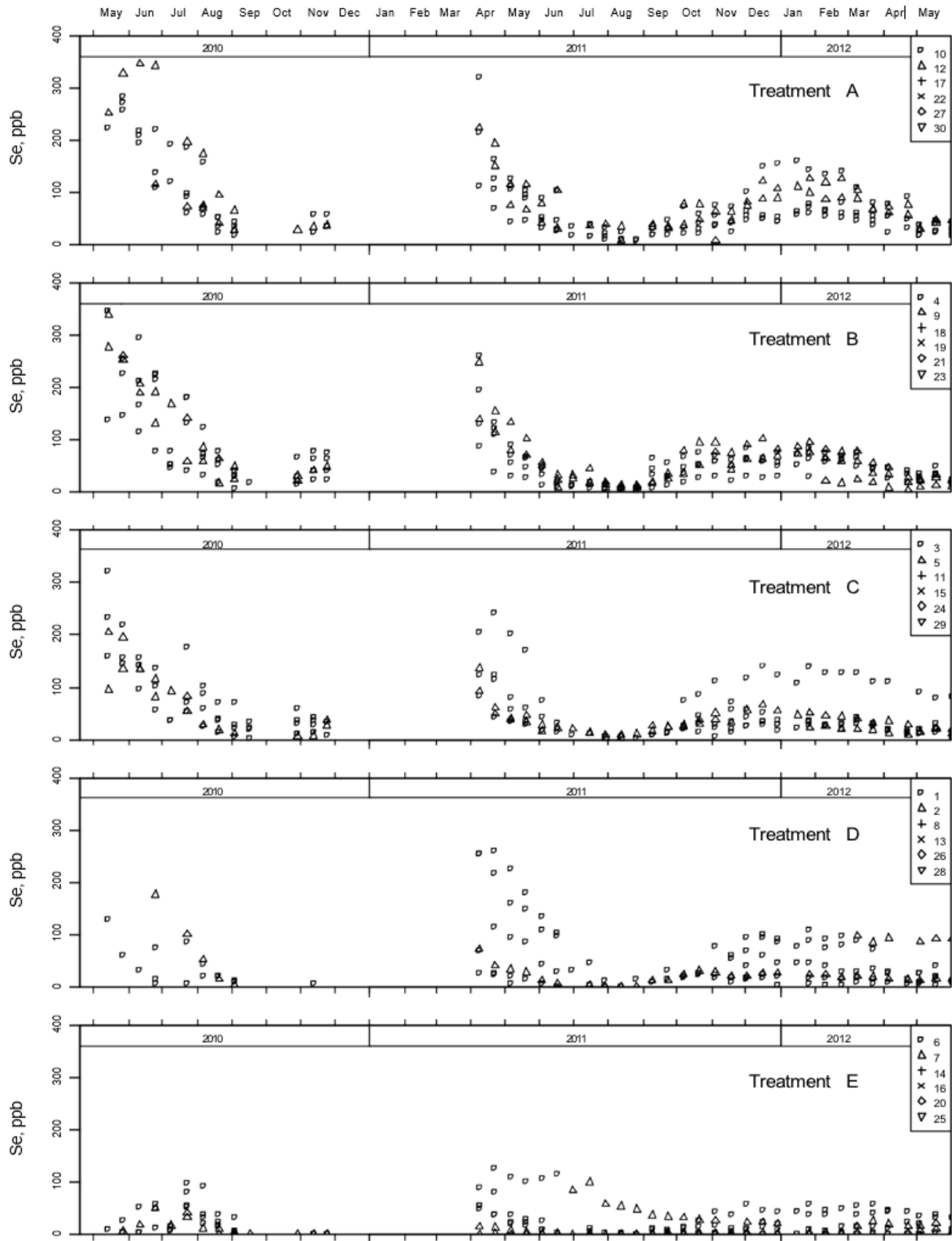


Figure 14: Raw Time Series of Se Concentrations Arranged by Treatment. Each plot shows replicates for different treatments. Treatment cells A= 0 in, B = 0.25 in, C = 2.25 in, D = 9 in and E = 18 in depth of Ferrihydrite.

### Statistical Analysis of Mean Concentrations

**Figure 15** shows the mean concentrations of the up to 6 replicates within each treatment (X symbols) and the 95% confidence limits on these concentrations calculated from sample standard errors and T values (based on n-1 degrees of freedom) for up to 6 replicates. The fitted line in all plots represents the means of Treatment A replicates (no ferrihydrite). Some error brackets are significantly larger than others, either due to more variability within replicates for that date (larger standard error) or due to fewer samples than 6 due to freezing or dry conditions (larger standard error and larger T statistic). Treating the zero-ferrihydrite mean as an unbiased estimate, the confidence range for the means of other treatments exceeding the zero-treatment mean curve decreases from Treatment B (0.25 inch ferrihydrite) to Treatment E (18 inch ferrihydrite). For treatment E, there are extensive periods when the confidence range for Se lies completely below the untreated mean Se curve. It is clear from these results that the mean Se concentrations decline in comparison to the Treatment A (control) values as the mass of ferrihydrite used increases.

### Se Fluxes

**Figure 16** shows time series of Se fluxes calculated using average discharge between sampling dates times the Se concentration at the end of the sampling period. The units are in grams/day of total Se. There appears to be no significant difference in flux between Treatments A and B, and in fact Treatment B was higher in Se flux in the initial three months of leaching, becoming more similar in 2011 and 2012 sampling. There is substantial decrease in Se loads for Treatments C, D, and E compared to both the Treatment A and B values. To a higher degree than the mean concentration plots, the fluxes demonstrate that Se fluxes are significantly lower in the Treatment C, D, and E lysimeters than in the untreated or lightly-treated lysimeters. **Figure 17** compares cumulative Se fluxes for the 5 treatments, again averaged for all replicates. Treatments A and B are, again, the highest in Se loads (112.8 and 149.8 g Se, respectively), with Treatment B being the highest based on elevated concentrations in the first 3 months of sampling. In later sampling, the A and B piles show no significant difference in their mean fluxes. Treatment C (76.8 g Se) is slightly lower in flux than treatment A and much less than B. Treatments D and E are both substantially lower (45.4 and 26.1 g, respectively). The mean Se flux for Treatment E at the end of the sampling period in 2012 was 76.9% lower than that of the untreated lysimeters.

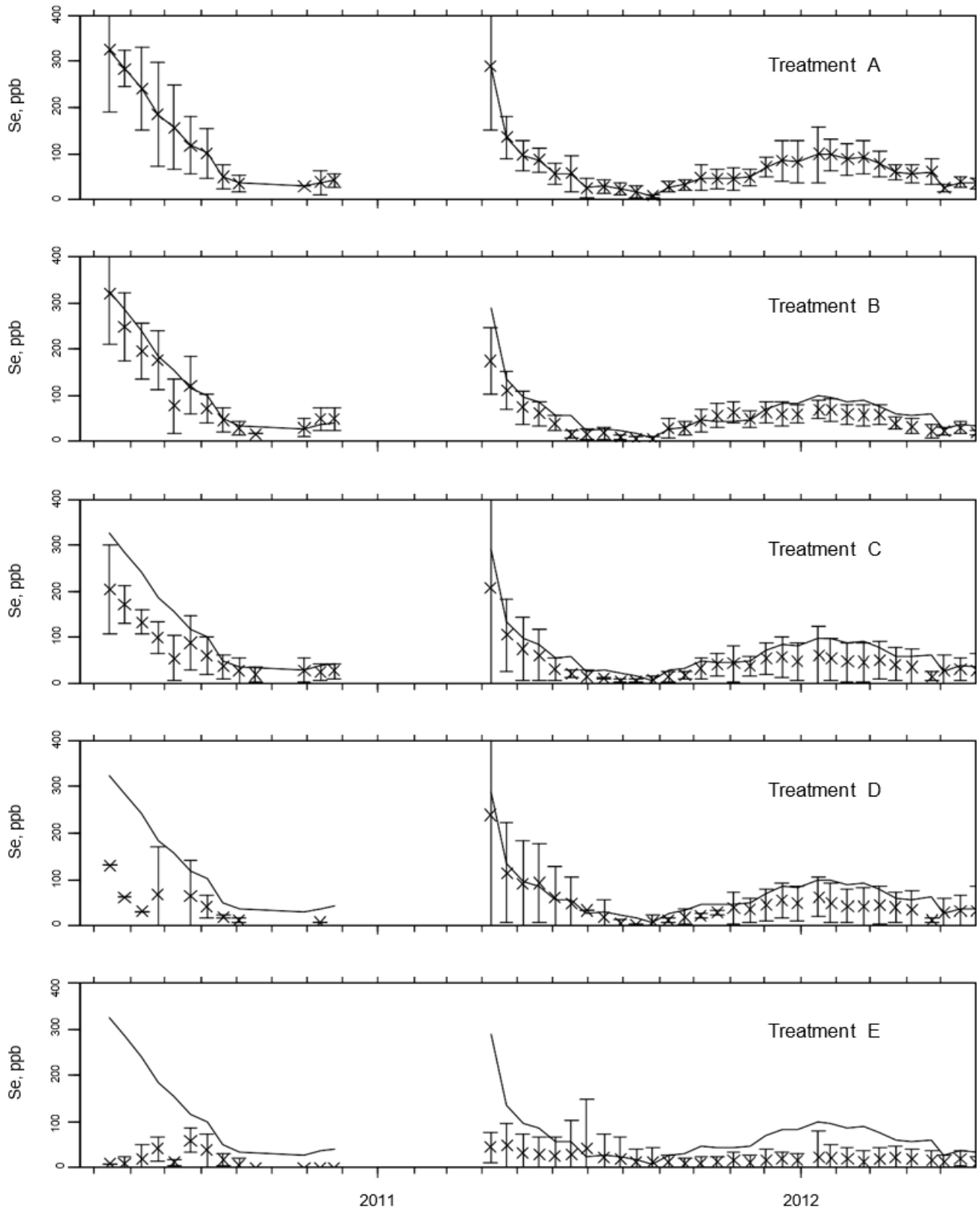


Figure 15: Time Series of Mean (X's) and Confidence Intervals (95%) for Se Concentrations of all Replicates within Treatment Classes (n=6 or less). Treatment cells A= 0 in, B = 0.25 in, C = 2.25 in, D = 9 in and E = 18 in depth of Ferrihydrite.

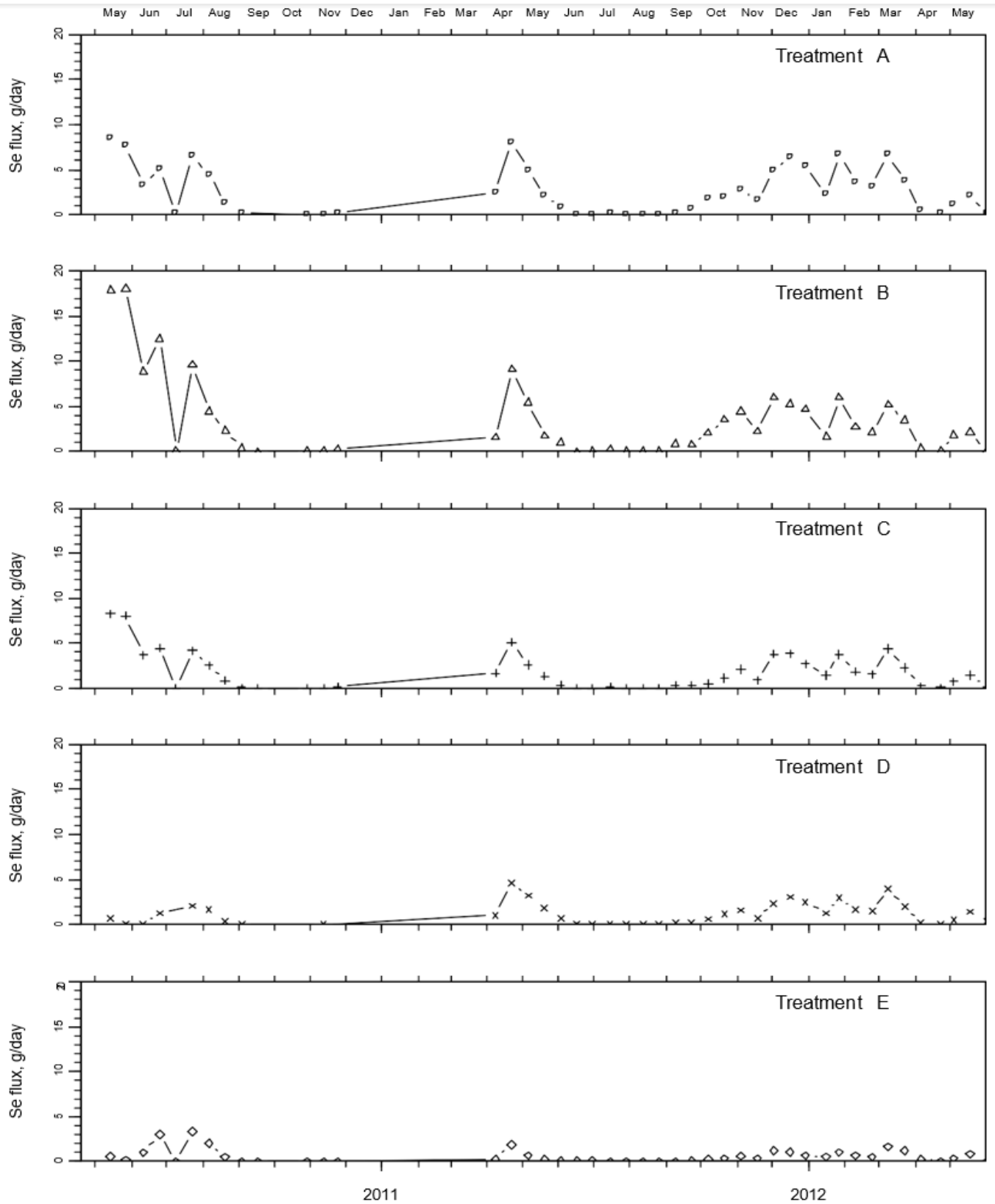
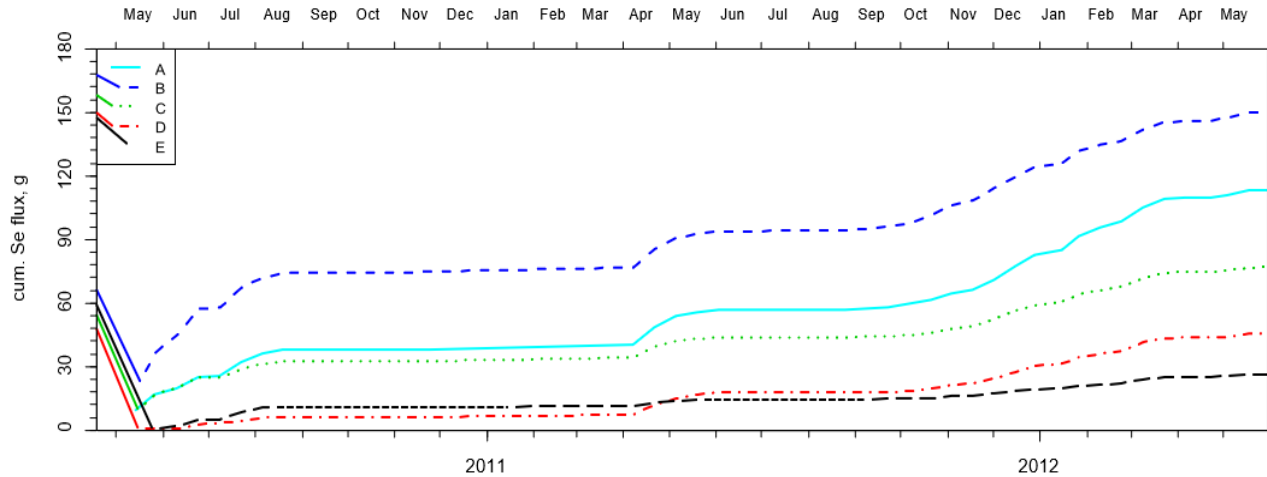


Figure 16: Time Series of Mean Se Flux (g/day) per Cell for each Treatment Class (n≤6). Treatment cells A= 0 in, B = 0.25 in, C = 2.25 in, D = 9 in and E = 18 in depth of Ferrihydrite.



**Figure 17: Cumulative Se Fluxes for the Five Ferrihydrite Treatments: A = 0 in, B = 0.25 in, C = 2.25 in, D = 9 in and E = 18 in depths.**

### Sequestration Mechanism

These results show conclusively that there was a very large reduction in Se flux for the lysimeters employing higher masses/thicknesses of ferrihydrite, compared to the untreated or lightly-treated cells. We attribute the reduction to adsorption of selenite and possibly selenate ion, although no redox estimates were obtained due to the batch method of sampling. There was not a proportional difference between the flux reduction of the 9-inch (59.8% reduction) and 18-inch (76.9% reduction) ferrihydrite layers. The use of thin ferrihydrite layers appeared to have little adsorption effect, and in fact early fluxes from the Treatment B piles were much higher than the controls.

### Replication and Variability

The variability of fluxes in all treatment replicates was not negligible, but within a limited range. There were minor outliers in Se concentration in both treatments C and D. However, at most sampling events for which a full number of replicates could be sampled, the standard errors were reasonably low. The largest sampling errors occurred when one or more of the replicates could not be sampled due to frozen plumbing or dry conditions. In general, the replication provides convincing evidence for reproducibility of both the Se-generating potential of untreated spoil and for its sequestration by adsorption using increasing masses of ferrihydrite.

The most surprising outcome was the elevated flux in the Treatment B piles compared to the control. Closer examination of the data indicates the leachate chemistry was similar between treatments, but more than twice the flow was collected in the B lysimeters than the A set. Nearly all of the increased flux occurred during the first three months of monitoring. The reason for this difference is not understood. After month three, flows of these two sets were similar for the remainder of the experiment. Sampling error of some type in flow measurement is a possibility.

## Se Mobility Observations

In all treatments, strong seasonality was observed in both Se concentrations and in flow rates. The "stair-step" appearance of Figure 8 underscores the episodic nature of Se fluxes. It may be speculated that, during winter conditions, infiltration into the spoil is at minimum rate but air ingress is continuous and encourages oxidation even while discharge of water is minimal, not only of mineral and organic fractions but also of selenite in sorbed form. The "slug" of elevated Se concentrations in spring may therefore represent flushing of over-winter reaction products. Strong Se flushes were observed both in early 2010 and 2011. In 2012, the flush occurred but at lower concentration than in the first two years. During drier seasons, both flow and concentration of Se drop to very low levels. The seasonality of Se discharge may offer water management options for addressing periods of high concentration.

## Practical Implications

The success of this sequestration trial suggests that an inexpensive waste material (ferric iron-rich mine drainage treatment sludge) could be an effective spoil amendment that could reduce and control dissolved Se outbreaks at mine scale. Organic-rich shale tends to be among the most sulfur- and selenium-rich overburden lithologies. It is often found stratigraphically above coal seams, which in combination with its diagnostic color, makes it amenable to selective handling during the mining process. Placing layers of ferrihydrite placed within and at the base of selectively-handled cells of organic shale may be a practical method for immobilizing a significant proportion of the Se flux for an entire surface mine. Scaling these results to much larger spoil masses will require testing and optimization of the technique. Nonetheless, a simple variant of this method yielded excellent sequestration in this investigation in cells for which the mass of ferrihydrite was sufficient. While many of the mean concentrations observed in Treatment E were higher than the 6 µg/L discharge limit (maximum 59.6 µg/L; mean 19.7 µg/L), these values are 4-6 times lower than in unamended spoil, and after July 2011, all values remained below 20 µg/L. While monitoring continues at this site, it may be hypothesized that much of the higher concentrations occurred in the first year or so of leaching. Given that such unamended spoil generates such extreme Se concentrations in leachate, the amenability of surface mine waters to Se management without active treatment may depend on such special handling techniques to control Se concentrations.

## Conclusions

This investigation was an experiment at field scale to test the effectiveness of a single basal ferrihydrite layer at reducing Se mobility in leachate derived from organic-rich shaly spoil. Thirty 24x16 foot lysimeters of identical construction, composition, and design, except for various thicknesses of ferrihydrite added, were monitored for 2.4 years on a bi-weekly basis. Key results include that:

- Time series of Se concentration and flux are highest during late winter and spring months, attributed both to spring flush of overwinter reaction products and to elevated recharge. Se fluxes are strongly seasonal, and winter/spring measurements of flux are critical to long-term accurate estimation
- In a trial of 4 different layer thicknesses of ferrihydrite and one control (no ferrihydrite), the three thickest ferrihydrite amendments showed significant reduction in Se fluxes from the

control, while the thinnest layer showed no reduction. The two thickest layers (9 and 18 inches) showed 59.4% and 76.9%, respectively, cumulative reduction in Se flux.

- All results were couched in terms of mean results for 6 replicates in each treatment class. The uncertainty due to variability in materials, construction, and hydrology of individual lysimeters was quantitatively assessed and considered within acceptable limits. The differences found in mean Se concentration and flux are considered to have a high probability of significance.

## Acknowledgements

This work was supported by funding from the US Office of Surface Mining to the senior author. The cooperation of Patriot Coal Company in constructing the lysimeters and providing site access was fundamental to the success of the project. Sampling assistance and laboratory chemical analyses were provided by REI Consultants, Beaver, West Virginia.

## References

- Diehl, S.F., Goldhaber, M.B., Koenig, A.E., Tuttle, M.L.W., and Ruppert, L.F. 2005. Concentration of arsenic, selenium, and other trace elements in pyrite in Appalachian coals of Alabama and Kentucky. Proceedings National Meeting of the American Society of Mining and Reclamation, p.283-301
- Dreher, G.B., and Finkelman, R.B., 1992. Selenium mobilization in a surface coal mine, Powder River Basin, Wyoming, USA. *Environmental Geology and Water Science*, 19: 155-167.
- Emerson, P., Skousen, J.G. and Ziemkiewicz, P.F. 2009. Survival and growth of hardwoods in brown versus gray sandstone on a surface mine in West Virginia. *J. Environ. Qual.* 38:1821-1829.
- Hawkins, J.W., 2004. Predictability of Surface Mine Spoil Hydrologic Properties in the Appalachian Plateau. *Ground Water* 42: 119–125.
- Huggins, F.E., Senior, C.L., Chu, P., Ladwig, K., and Huffman, G.P. 2007. Selenium and arsenic speciation in fly ash from full-scale coal-burning utility plants. *Environ. Sci. Technol.* 41:3284-3289
- Hyun, S., Burns, P.E., Murarka, I., and Lee, L.S. 2006. Selenium (IV) and (VI) sorption by solid surrounding fly ash management facilities. *Vadose Zone J.* 5:1110-1118
- Maher, T.P., and Donovan, J.J., 1997. Double-flow behavior observed in well tests of an extremely heterogeneous mine-spoil aquifer. *Engineering Geology*, 5: 83-99 (17)
- Merrill, D.T., P.M. Maroney, and Parker, D.S. 1985. Trace element removal by coprecipitation with amorphous iron oxyhydroxide: engineering evaluation. Electric Power Research Institute Coal Combustion Systems Division, Report EPRI, CS 4087, Palo Alto, CA.

- Mullenex, R.H. 2005. Stratigraphic distribution of selenium in upper Kanawha-lower Allegheny formation strata at a location in southern West Virginia. The 23<sup>rd</sup> Annual International Pittsburgh Coal Conference, Pittsburgh, PA, Poster.
- Naftz, D.L., and Rice, J., 1989. Geochemical processes controlling selenium in ground water after mining, Powder River Basin, Wyoming, USA. *Applied Geochemistry*, 4: 565-576.
- Pumure, I, Renton, J.J., and Smart, R.B. 2010. Ultrasonic extraction of arsenic and selenium from rocks associated with mountaintop removal/valley fills coal mining: estimation of bioaccessible concentrations. *Chemosphere* 78:1295-1300
- Roy, M. 2005. A detailed sequential extraction study of selenium in coal and coal-associated strata from a coal mine in West Virginia. M.S. Thesis, Department of Geology and Geography, West Virginia University, Morgantown, WV, USA. 103 pp.
- Su, C., and Suarez, D.L. 2001. Selenate and selenite sorption on iron oxides: an infrared and electrophoretic study. *Soil Sci Soc Am J* 64:101-111.
- Vesper, D.J., Roy, M., and Rhoads, C.J. 2008. Selenium distribution and mode of occurrence in the Kanawha formation, southern West Virginia, U.S.A., *Int J Coal Geol* 73:237-249
- Zhang, P., and Sparks, D.L. 1990. Kinetics of selenate and selenite adsorption/desorption at the goethite/water interface. *Environ. Sci. Technol.*, 24:1848-1856
- Ziemkiewicz, P.F., O'Neal, M. and Lovett, R.J. 2011. Selenium leaching kinetics and in-situ control. *Mine Water Environ* 30: 141–150.
- Ziemkiewicz, P.F. and Lovett, R.J., 2012. Determination of natural attenuation of selenium at a coal-mining complex in West Virginia. Proceedings, 9th International Conference on Acid rock drainage, Ottawa, Ontario Canada. 20-26 May 2012.

## **Task 3: Natural Attenuation of TDS in Mountaintop Mines**

### **Executive Summary**

Mountain Top Mining (MTM) is used to extract multiple coal seams in difficult terrain. Valley fills are created from the associated mine spoil and placed at the heads of hollows. Although a large amount of research has been performed on MTM and its effects, specific ion concentrations of valley fill discharges and how they are related to overburden geology and valley fill age has not been well-studied. This study researched the effects of valley fill age, flow regime, and type of coal seam mined.

Water samples, flow, and field data were collected at two southern West Virginia mine complexes during a low flow period and three mine complexes during a high flow event. Samples were collected from the toes of 20 valley fills during the low flow sampling event and 38 fills during the high flow sampling event. Data were sorted by valley fill age, sampling event, and coal seam mined, and analyzed using regression analysis.

Sulfate, bicarbonate, calcium, and magnesium made up the largest percentage of TDS. Sulfate, bicarbonate, and magnesium increased for all fills and during high and low flow events, while calcium showed a slight decrease in concentration over time during high flow. Selenium concentrations followed a similar trend to calcium. Selenium concentrations had the greatest correlation between valley fill age and parameter concentrations. Overall, TDS concentrations increased with time, likely due to continued leaching of salts within the valley fills.

Parameter concentrations were also compared against coal seams mined. Concentrations from Upper Kanawha (UK) mines increased over time for sulfate,  $\text{HCO}_3$ , and TDS. These same parameters decreased over time for LK mines. Magnesium and calcium increased over time regardless of coal seam mined. Selenium had the greatest correlation between fill age and concentrations of all coal seam comparisons. UK mines declined rapidly beginning 7 years after construction and had a 91% reduction after 30 years and LK mines decreased by 93%.

With the exception of selenium, the low  $R^2$  values found in the current data do not indicate that a noteworthy correlation between valley fill age and parameter concentrations exist. Subsequent research could be conducted by increasing the number of sampled fills, gathering additional data from existing datasets, or widening the geographical area to be more inclusive of regional geology. Increasing the size of the study area also may show that the data trends found from these fills are vastly different than other fills.

### **Introduction**

Thin seams of coal are extracted in southern West Virginia (WV) using a process known as Mountain Top Mining (MTM). Excess spoil from this process is placed in constructed valley fills. Valley fills are typically placed in the heads of hollows where headwater streams are formed. A great deal of research has been performed on various aspects of MTM and its effects. However, there is little documented research related to specific ion concentrations of valley fill toe discharges and how they are related to

overburden geology and valley fill age. Ions found in the largest concentrations; Calcium (Ca), Sodium (Na), Magnesium (Mg), Sulfate (SO<sub>4</sub>), Bicarbonate (HCO<sub>3</sub>), and Chloride (Cl<sup>-</sup>), constitute the overwhelming majority of Total Dissolved Solids (TDS) and Electrical Conductivity (EC) in this region of Appalachia. Compliance with selenium (Se) criteria has also become a potential regulatory issue in the southern WV coalfields. An explanation of these chemical profiles is particularly important in light of West Virginia's new narrative water quality standard for TDS. It was our hypothesis that ion composition and concentration were functions of overburden geology and valley fill age. We expected that ion leaching would be relatively rapid, given the high permeability of these valley fills.

Previous research has estimated the longevity of specific mine pollutants. Investigations of surface mine discharges have shown that acidic water may be released at a consistent level for 10 to 20 years (Meek, 1996), while Wood et al. (1999) determined that surface mines attenuated much more quickly than underground mines. However, underground mine discharges are more difficult to predict. Younger (1997) estimated that acidic drainage may continue for 10 to 100 years, dependent upon hydrologic factors, pyrite reaction rate, and amount of pyrite. Other researchers have found that the worst pollution occurs within the first 40 years after mine closure (Wood et al., 1999) and that several decades must elapse before water quality will improve significantly (Jones et al., 1994).

Research by West Virginia University has studied the longevity of mine water pollutants from underground mines in the Pittsburgh and Upper Freeport coal seams. Mack et al. (2010) found that acidity decreased, on average, 80% over 40 years (**Figure 18**). Demchak (2005) studied 20 underground mines and found that acidity, metals, and sulfate decreased 50-80% over 32 years. A partially flooded Pittsburgh seam mine was also studied by Demchak (2005). She researched changes in sulfate concentrations over time since mining was completed and found that sulfate concentrations showed a very rapid rate of exponential decline (**Figure 19**).

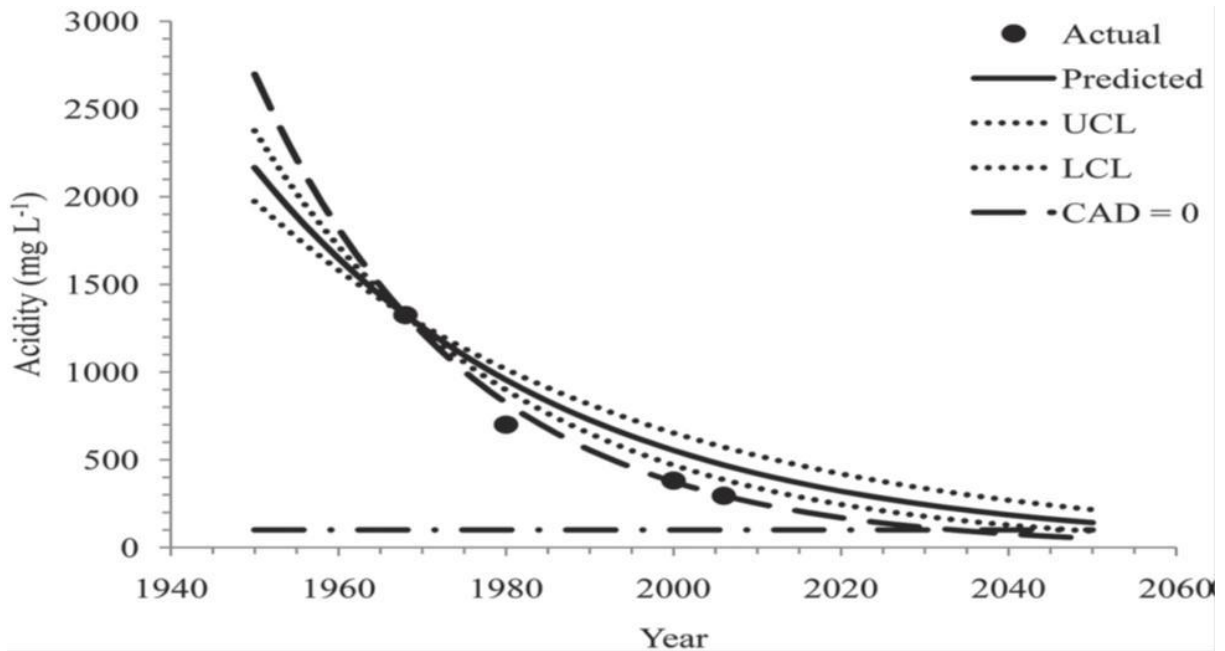


Figure 18: Acidity (mg/L) for Upper Freeport sites extrapolated to the year 2050. Horizontal dashed line represents the cutoff acidity to begin passive treatment (100 mg/L). CAD, cumulative average difference; LCL, lower confidence limit; UCL, upper confidence

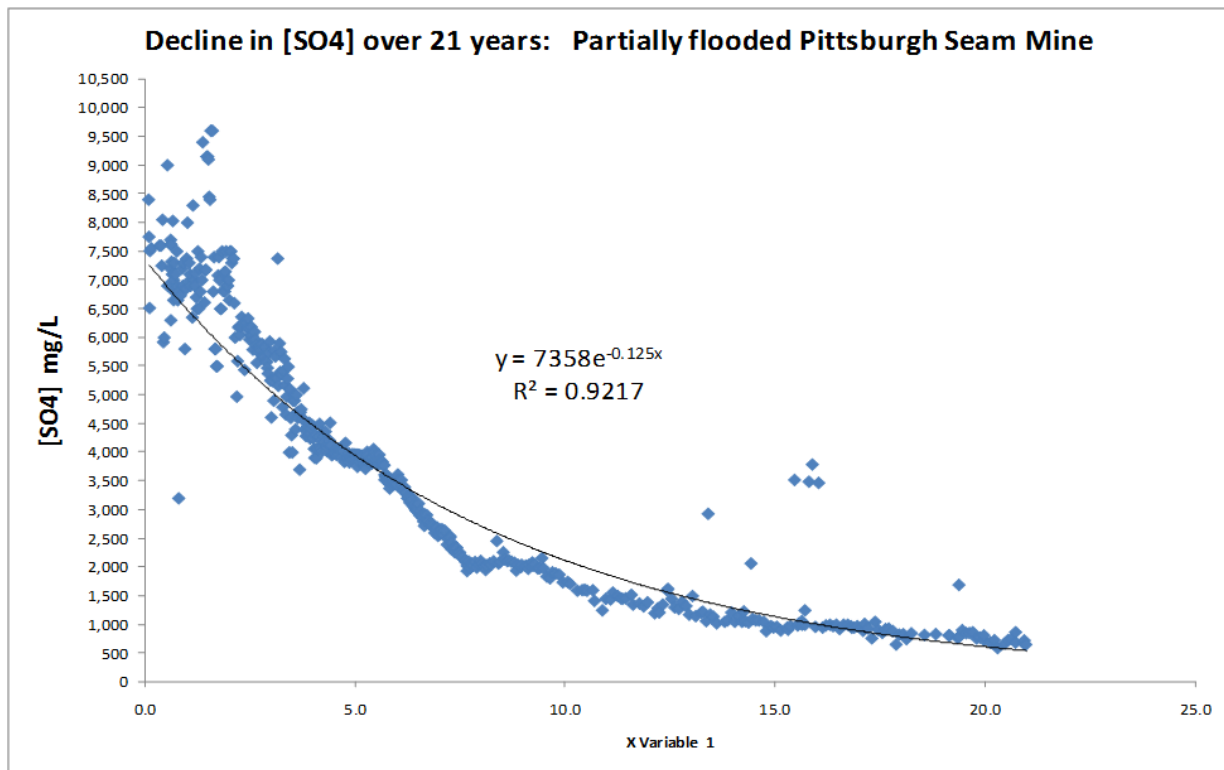
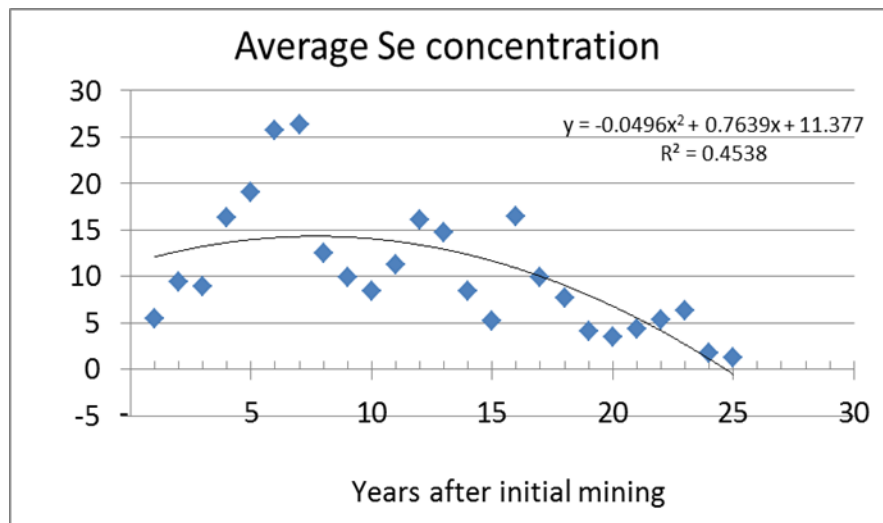


Figure 19: Sulfate decline during 21 years after flooding of mine in the Pittsburgh coal seam (Demchak, 2005). The x-axis is years after mining completion.

Selenium concentrations also are often associated with coal seams (Mullenex, 2005). Roy (2005) and Vesper et al. (2008) determined that potentially damaging levels of selenium can be found associated with carbon-rich strata. However, the natural rate of decline of Se without treatment has not been well-studied. Research by the WV Water Research Institute has estimated the rate of decline for selenium. **Figure 20** shows changes in selenium concentrations as a function of time after mining began. Selenium concentrations began to decline approximately eight years after mining began and reached a concentration of less than 1 µg/L after 25 years (WRI unpublished data, 2010).

Ziemkiewicz et al. (2011) compared Se leaching rates from coal mine tailings treated with FeOOH to those that were untreated. Untreated coal tailings released Se at a rate of 0.06% of the total leachable Se per day while tailings treated with FeOOH had a leaching rate of 0.016% per day. Natural attenuation of Se to 5 µg/L, (chronic aquatic life toxicity standard), would take 4.7 years.



**Figure 20: Average Se concentrations over time.**

## Materials and Methods

The West Virginia Water Research Institute conducted field sampling events at two southern West Virginia mine complexes during a low flow period and three mine complexes during a high flow event. These large complexes have been in existence for decades and have numerous valley fills of different sizes and ages. Effluent samples were collected from the toes of 20 valley fills during the low flow sampling event and 38 fills during the high flow sampling event (**Figure 21**).

Individual fills were selected to meet the criteria listed in **Table 9**. For the purposes of this study, Lower Allegheny/Upper Kanawha coals include the 5 Block, Stockton, and Coalburg seams and the Lower Kanawha coals are all coal seams below the Coalburg. **Table 10** describes the field and lab data collected for each valley fill.

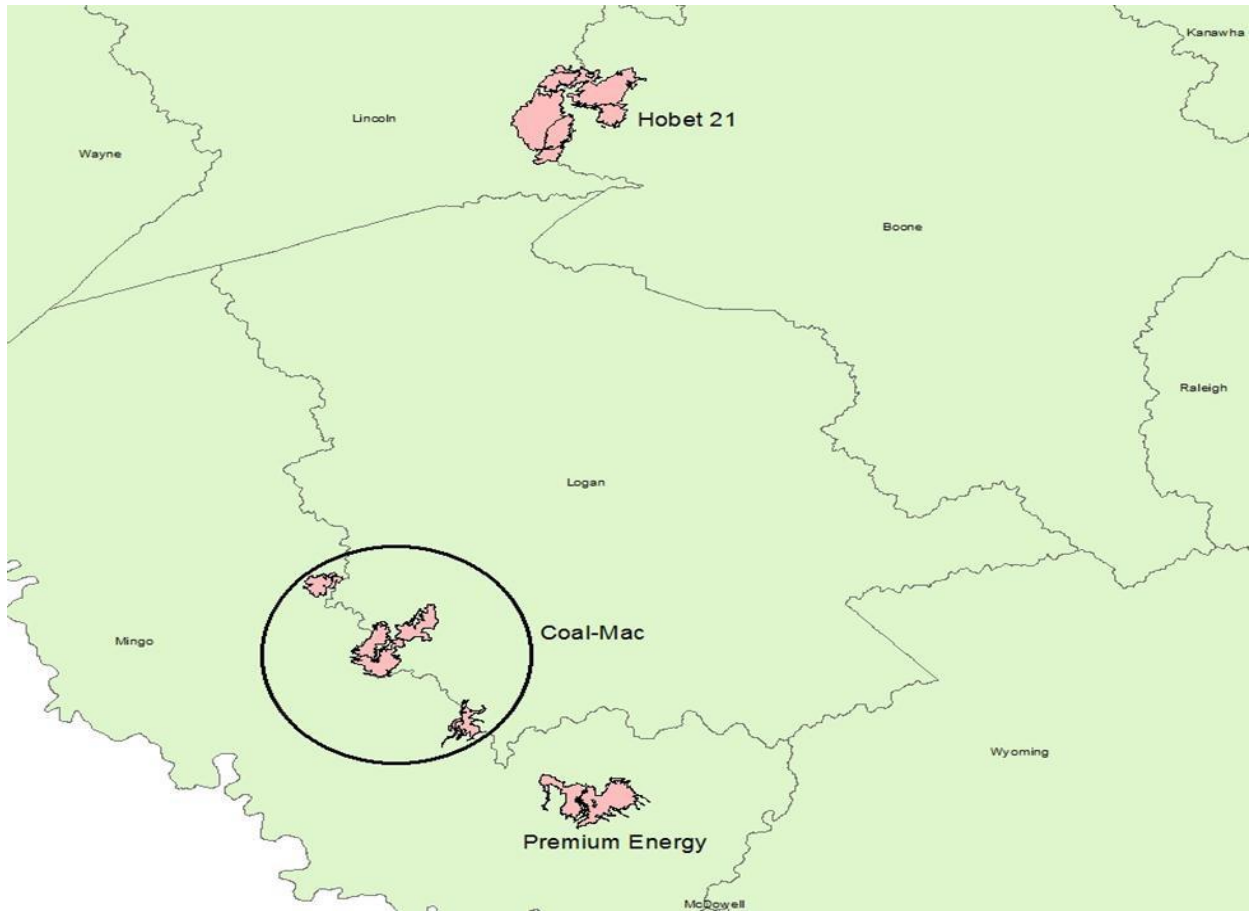


Figure 21: Mine sites that were sampled during two sampling events.

Table 9: Criteria Used for Valley Fill Selection

Criteria	Criteria units	# of fills
Valley Fill Age	0-5 yrs	5
	6-10 yrs	17
	11-15 yrs	8
	16-25 yrs	5
	25+ yrs	6
Coal seams mined	Lower Allegheny / Upper Kanawha (UK)	20
	Lower Kanawha (LK)	21

**Table 10: Information taken at each Valley Fill Sample Point**

Sample type	Number of samples	Field data	Lab data
Valley fill toe	58	Flow, EC, TDS, pH, DO, Temperature	Fe, Al, Mn, Ca, Mg, Na, Cl, HCO <sub>3</sub> , Se, SO <sub>4</sub>

EC = electrical conductivity; TDS = total dissolved solids; DO = dissolved oxygen

Field and lab data were collected and analyzed using protocols approved by the US EPA. Flow values were determined using a Marsh-McBirney Flo-Mate and the cross-sectional area of the discharge. Flows were taken at the toe of each valley fill after all discharge had been channelized. The impacts from changes in flow on all sampled parameters are discussed in greater detail within the Results and Discussion section of this report.

Groundwater above the channelization point was not captured because a representative sample could not be obtained at any point above the toe of the fill. Groundwater travel times could not be estimated due to the inability to determine flow above the toe of the fill. As such, they are not included in this report.

All other field parameters were determined by using an YSI 556 multi-probe. All water samples were sent to REI Consultants Laboratory in Beaver, West Virginia for analysis. Dissolved Al, Fe, Mn, Ca, Mg, and Na were determined using EPA method 200.7. Total Cl and SO<sub>4</sub> were found using method number E300.0 and Total HCO<sub>3</sub> was determined using SM2320B. Both total and dissolved Se were ascertained using method SM3114B. Data were sorted by valley fill age, sampling event, and coal seam mined. The highest R<sup>2</sup> values were used to determine the amount of correlation between parameter concentrations, valley fill age, and coal seam mined for Sample 1 and 2 (**Table 11**). A single factor ANOVA was run for each set of relationships to determine significance. All relationships were significant at an alpha of 0.05.

Table 11: R2 Values for all Parameters and Comparisons

Parameter	Low Flow vs. VF age	High Flow vs. VF age	All fills vs. VF age	UK vs. VF age	LK vs. VF age
TDS	Polynomial 0.242	Exponential 0.102	Exponential 0.179	Power 0.199	Polynomial 0.044
SO <sub>4</sub>	Power 0.329	Polynomial 0.105	Exponential 0.201	Power 0.0263	Polynomial 0.049
HCO <sub>3</sub>	Power 0.047	Power 0.030	Exponential 0.070	Power 0.022	Polynomial 0.0343
Ca	Polynomial 0.052	Polynomial 0.004	Polynomial 0.005	Power 0.032	Power 0.036
Mg	Power 0.386	Polynomial 0.255	Power 0.301	Power 0.347	Power 0.094
Se	Polynomial 0.717	Linear 0.576	Exponential 0.136	Exponential 0.440	Logarithmic 0.452

UK = Upper Kanawha coal seams, LK = Lower Kanawha coal seams

## Results and Discussion

Nine ions (HCO<sub>3</sub>, SO<sub>4</sub>, Cl, Fe, Mn, Ca, Mg, Na, and Se) were used as indicators of change in TDS concentrations over time. Figure 5 details percentage of contribution of each ion to TDS. The four ions that had the largest percent contribution to TDS, as well as Se, were plotted as a function of valley fill age, as were EC, TDS, and pH. The data were analyzed using regression analysis.

## Contributing TDS Ions (fill average)

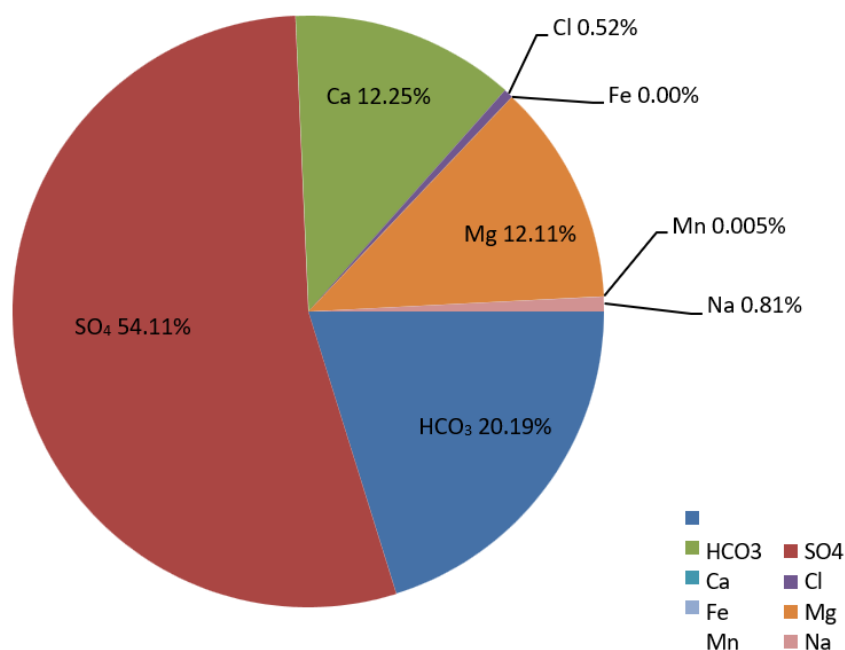


Figure 22: Major Ions Contributing to TDS

### Effects on ion concentrations due to valley fill age

All parameters were graphed as a function of valley fill age. Data from both sample times were combined to determine the overall impact of valley fill age on the parameter. The data was also split into a high and low flow sampling event to determine if flow impacted parameter concentrations.

#### Sulfate

Sulfate concentrations showed a slight increase as valley fill age increased (**Figure 23**). However, very little correlation was found between sulfate and fill age (**Table 11**). Sulfate concentrations also showed an increase over time under both high and low flow conditions (**Figure 24**). A possible explanation of increased sulfate is a lack of data for fills age 0-5 years compared to other age classes. Sulfate concentrations could be greater in the first five years after valley fill completion, which could change the shape of the curve from an increasing trend to a decreasing trend. Sulfate increased more rapidly during the low flow sampling event and had a higher  $R^2$  value. However, fairly low  $R^2$  values (**Table 11**) at both high and low flow show that very little correlation between sulfate and valley fill age exists and that flow has very little effect on sulfate concentrations.

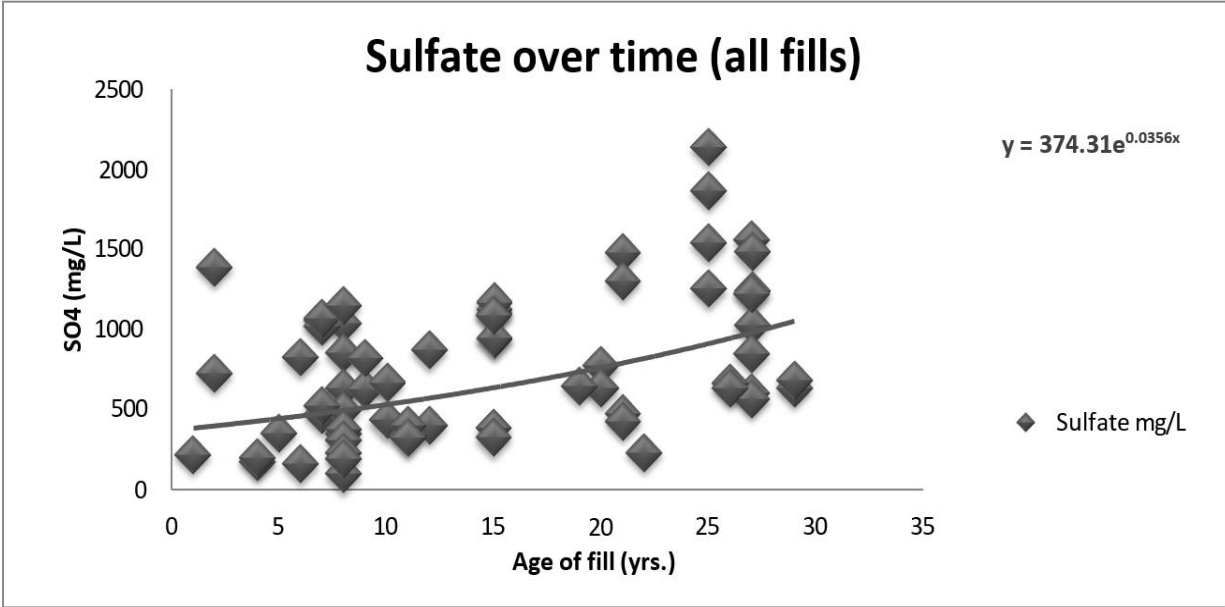


Figure 23: Sulfate concentrations as a function of valley fill age.

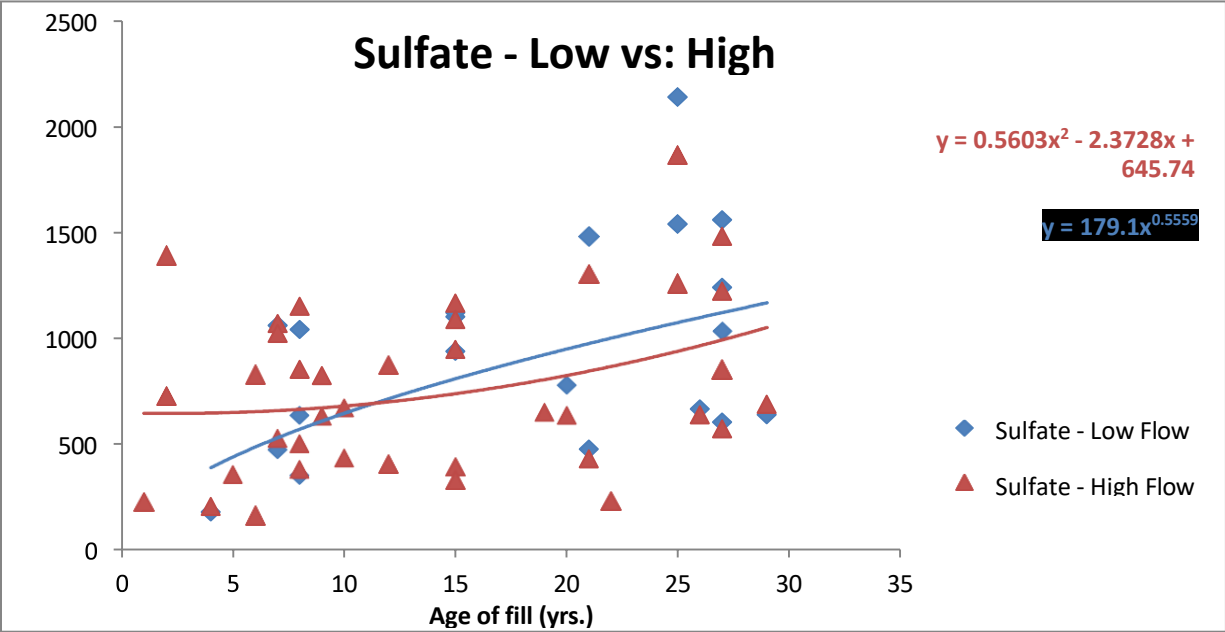


Figure 24: Sulfate concentrations as a function of valley fill age and flow regime.

### HCO<sub>3</sub>

Similar to sulfate, HCO<sub>3</sub> concentrations increased over time (**Figures 25 and 26**). However, HCO<sub>3</sub> increased more slowly than sulfate. Low R<sup>2</sup> values indicated a weak increasing HCO<sub>3</sub> concentration for all fills as well as at both flow regimes (**Table 11**). Low correlation values were found between HCO<sub>3</sub> concentrations and both flow regime and valley fill age. Production of alkalinity increased past the age of the oldest fill. However, a 29 year-old valley fill with an HCO<sub>3</sub> concentration of 1,060 mg/L significantly affected the rate of HCO<sub>3</sub> increase. A decline in HCO<sub>3</sub> production is expected as alkaline material continues to leach from the fills.

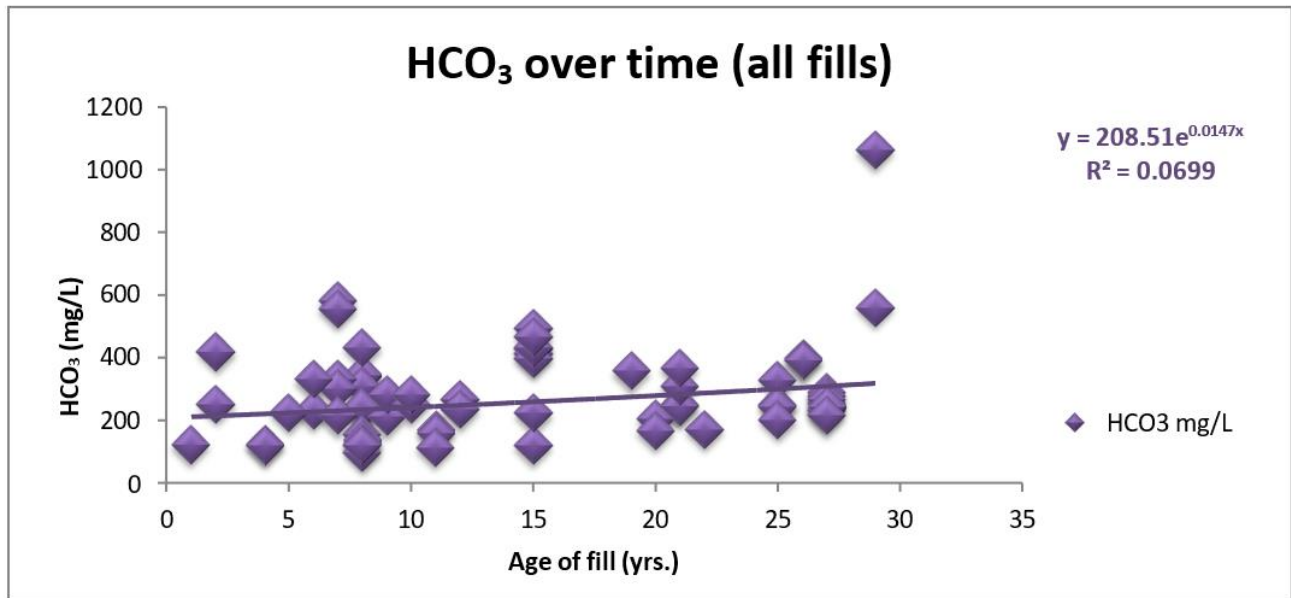


Figure 25: HCO<sub>3</sub> concentrations as a function of valley fill age

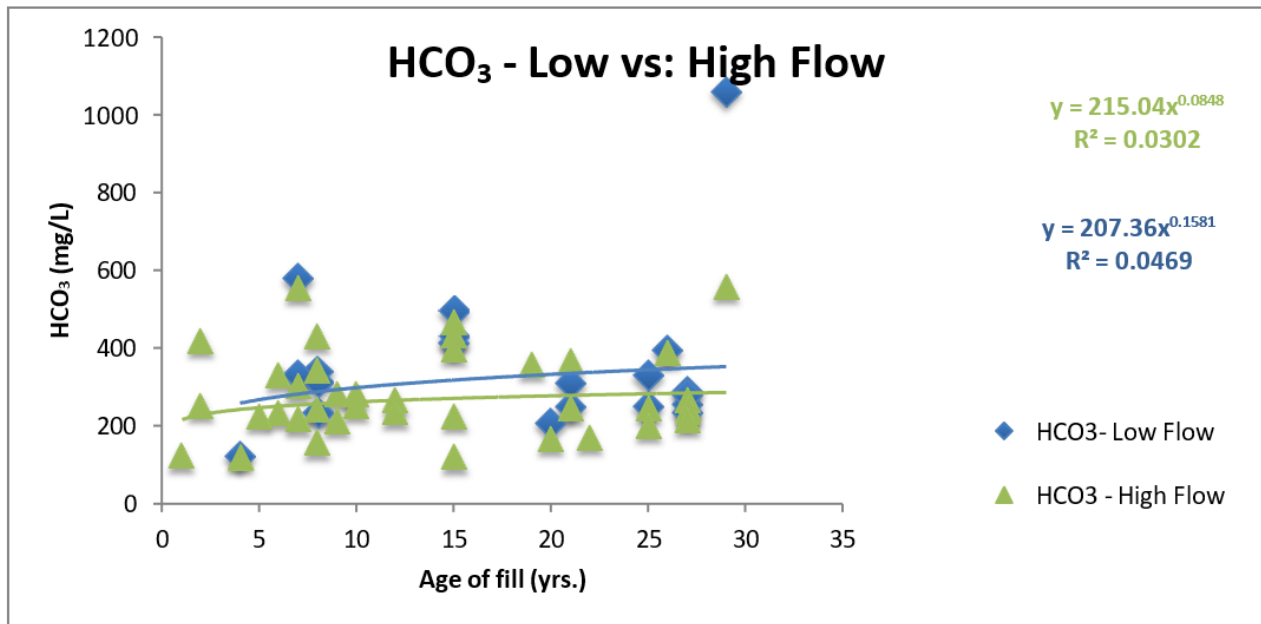


Figure 26: HCO<sub>3</sub> concentrations as a function of valley fill age and flow regime.

Magnesium

Magnesium (Mg) concentrations contributed approximately 12% to the makeup of TDS (Figure 22). Concentrations ranged from approximately 35 to 450 mg/L (Figures 27 and 28). Concentrations increased past the age of the oldest fill regardless of valley fill age or flow regime. This trend indicates that flushing of magnesium minerals continues to occur past 30 years. However, R<sup>2</sup> values for all fills (0.30), low flow (0.39), and high flow (0.26) indicate a moderate correlation between fill age and Mg concentrations. Concentrations likely will begin to decrease as the fills age due to a lack of easily weathered material.

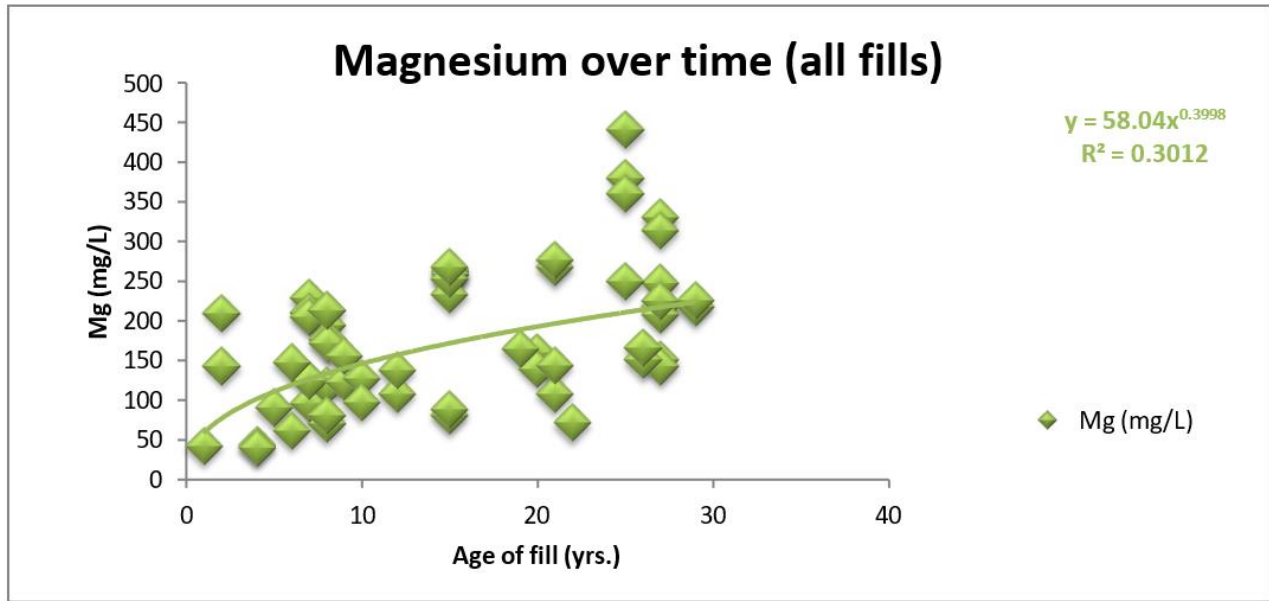


Figure 27: Magnesium concentrations as a function of valley fill age.

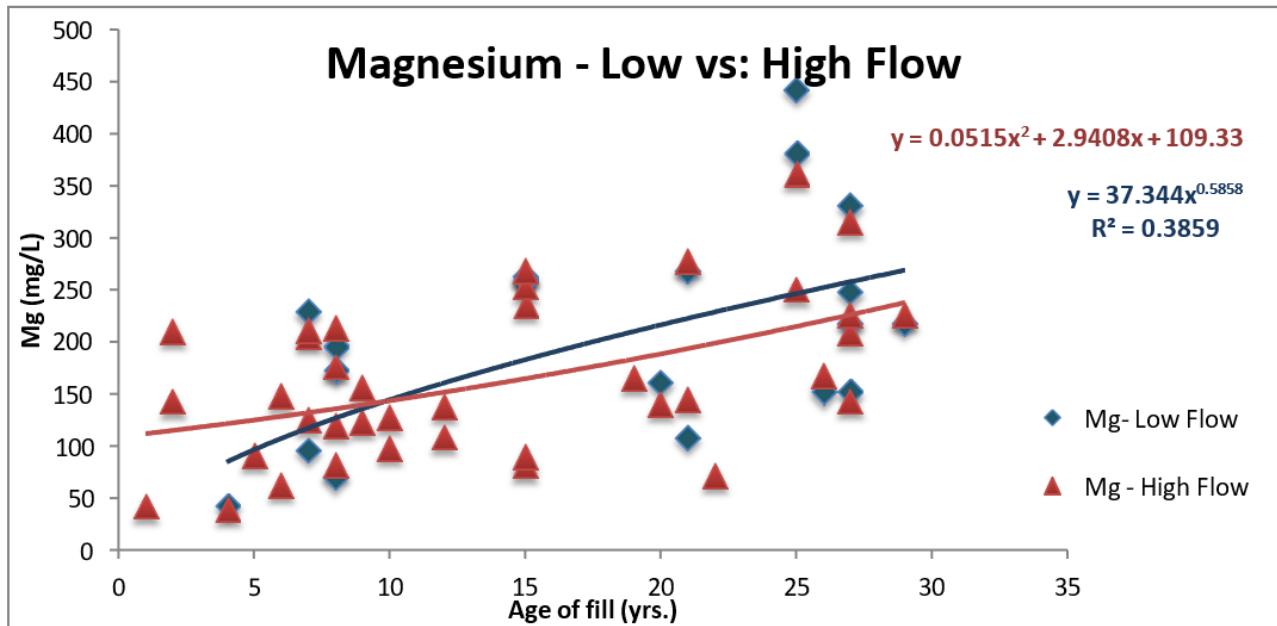


Figure 28: Magnesium concentrations as a function of valley fill age and flow regime.

## Calcium

Calcium also contributed roughly 12% of the total makeup of TDS (**Figure 22**). Calcium concentrations ranged from 75 to 415 mg/L. Concentrations for all fills began to stabilize at 18 years after valley fill construction and 16 years for the low flow sample. Concentrations began to decrease 18 years after construction and 20 years after construction, respectively (**Figures 29 and 30**). A combination of low flow and low solubility could explain why the observed decrease did not begin until fills reached at least 18 years old. The high flow sample showed a more consistent decrease as valley fill age increased.

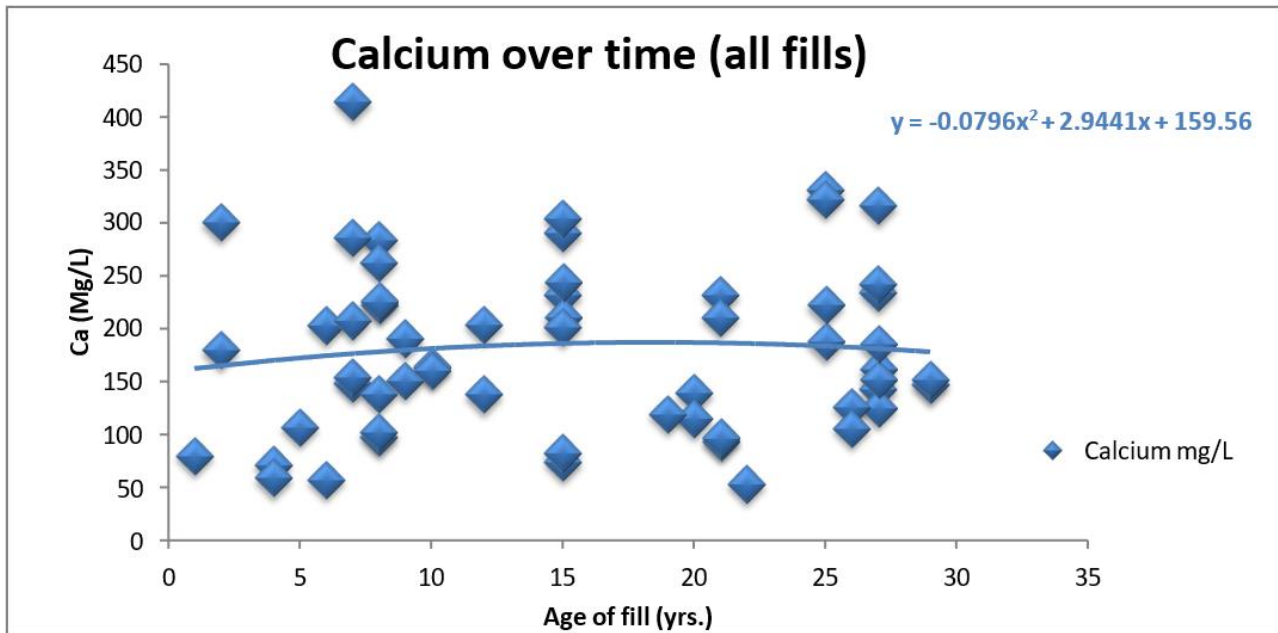


Figure 29: Calcium concentrations as a function of valley fill age.

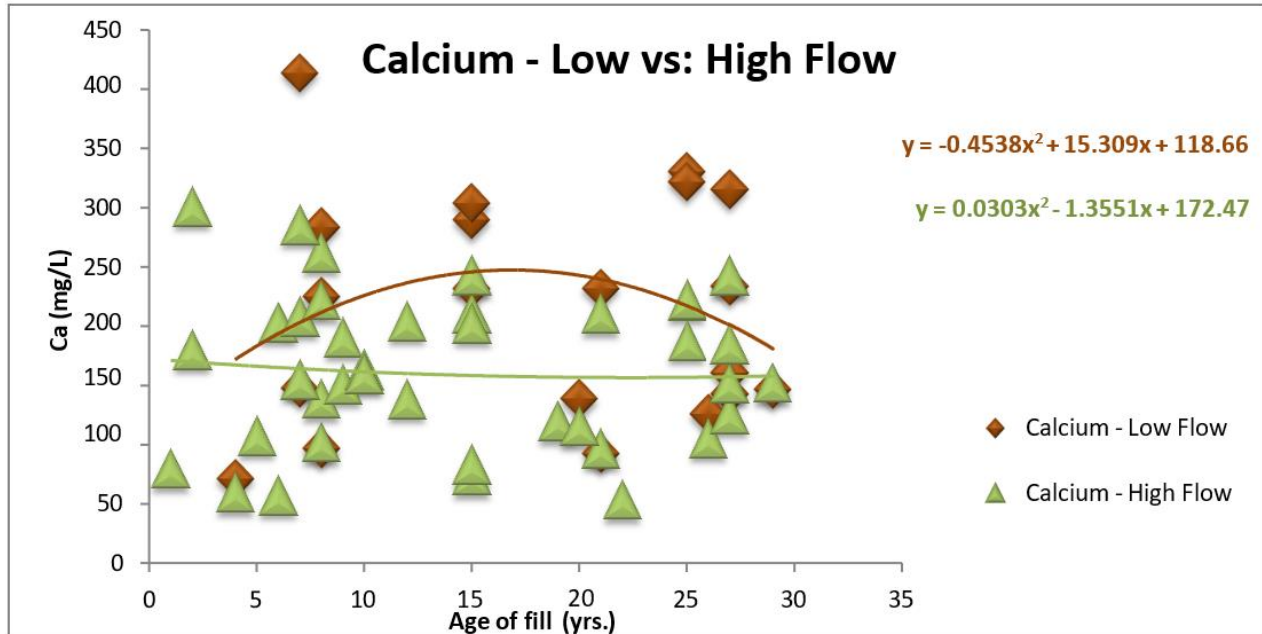


Figure 30: Calcium concentrations as a function of valley fill age and flow regime.

Selenium

Although selenium is not a large contributor to TDS in this region, it is a regulated parameter in mine discharges. Selenium concentrations from all fills and from the low flow sampling event decreased over time (**Figures 31 and 32**). However, a rapid increase in selenium concentrations was observed during the high flow sample. This is likely due to a limited number of data points, as the majority of low flow samples had selenium concentrations below detectable limits. When the data was categorized by flow, selenium concentrations correlated fairly well with valley fill age at both high and low flows ( $R^2$  values of 0.57 and 0.72, respectively) (**Figure 32**). Further sampling of valley fills during high flow events is expected to yield a similar trend to those seen during low flow events.

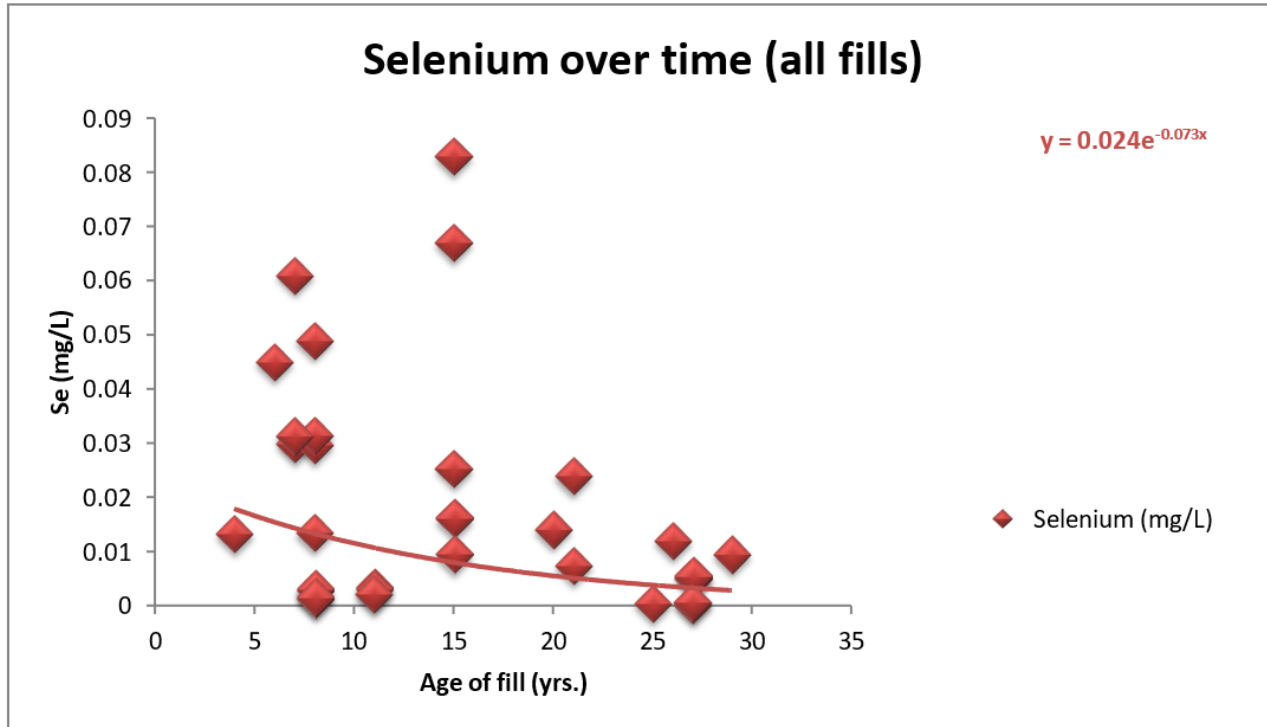


Figure 31: Selenium concentrations as a function of valley fill age.

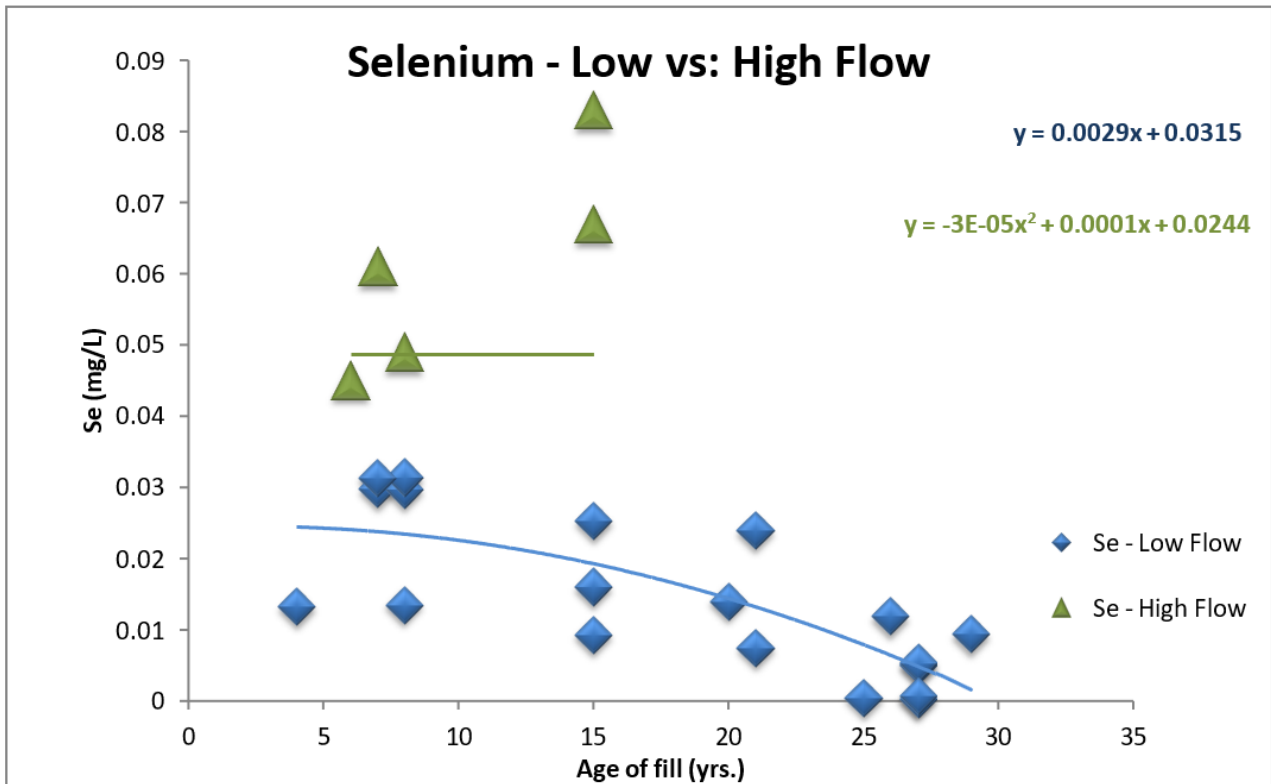


Figure 32: Selenium concentrations as a function of valley fill age and flow regime.

## TDS

TDS concentrations from all fills and the high flow sampling event increased as the valley fills aged (**Figures 33 and 34**). A steady pulse of TDS constituents is being released during high flow events. Concentrations also increased during low flow conditions. However, TDS concentrations leveled off 19 years after fill construction and began to decrease 21 years after construction. Leaching appears to be continuing within these fills, likely due to continued exposure of previously unweathered material to oxygen and water. However, concentrations likely will decrease as available TDS constituents are leached from the valley fill.

R<sup>2</sup> values were nearly identical when comparing all fills and data collected during high flows (**Table 11**). Higher flows typically cause higher TDS concentrations because larger amounts of certain TDS constituents, such as sulfate and selenium, are flushed out of the valley fill. Sulfate makes up approximately 54% of total TDS concentrations (**Figure 21**) and is highly soluble. High flow events would leach more sulfate from the valley fill, which would increase overall TDS concentrations.

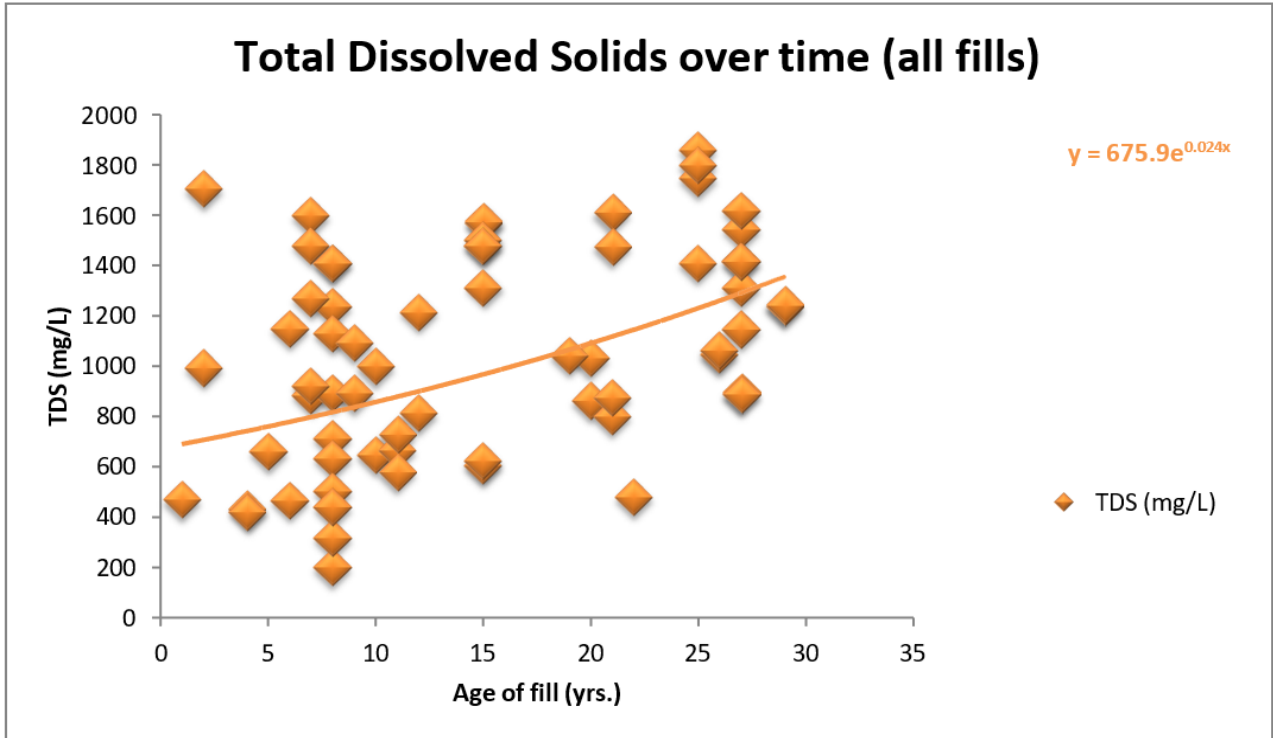


Figure 33: TDS concentrations as a function of valley fill age.

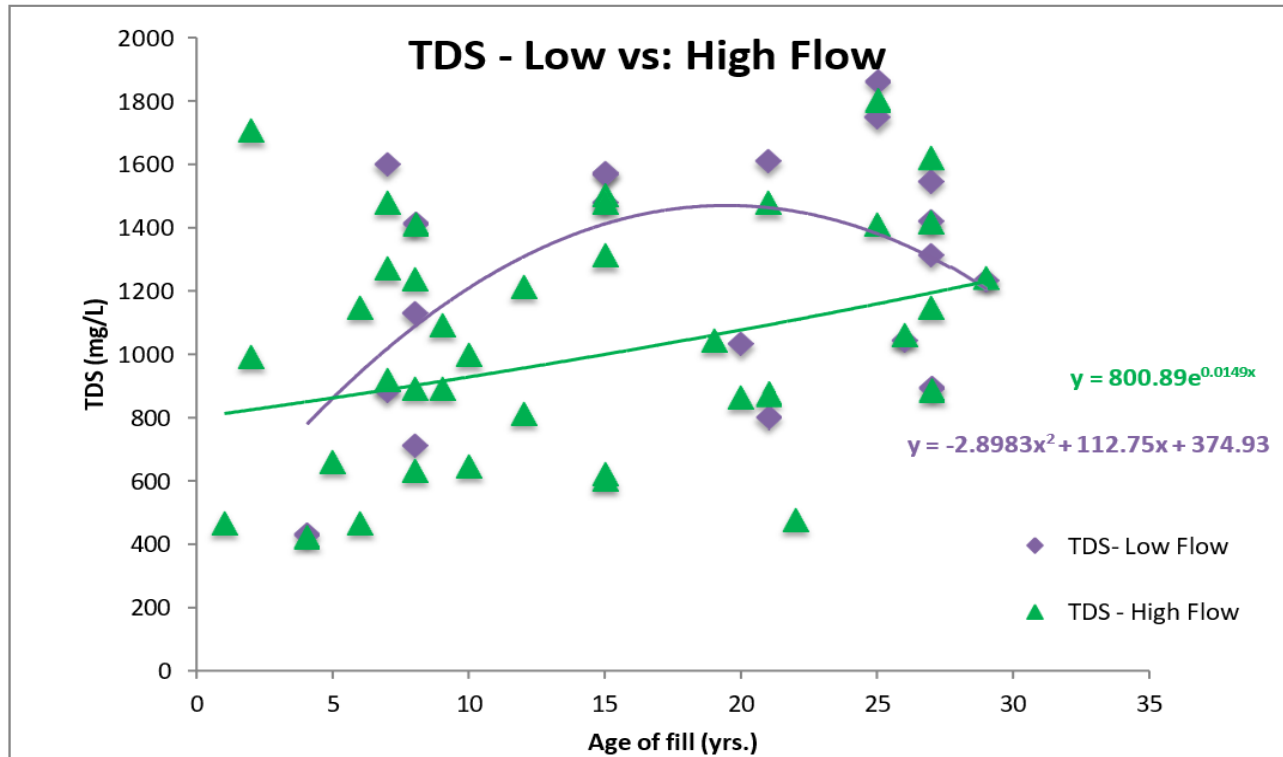


Figure 34: TDS concentrations as a function of valley fill age and flow regime.

### Effects on ion concentrations due to coal seams mined

SO<sub>4</sub>, HCO<sub>3</sub>, Mg, Ca, Se, and TDS concentrations were also compared against coal seam geology. Parameter concentrations from two Upper Kanawha (UK) and two Lower Kanawha (LK) mines were plotted as a function of valley fill age. The data were analyzed using similar methods to those used for flow regime comparisons.

#### Sulfate

Sulfate concentrations showed very little correlation to fill age regardless of coal seams mined (**Table 11**). Coal seams that were deposited more recently (UK) showed increased sulfate concentrations over time, while the opposite was true for older coals (LK) (**Figure 35**). Fills older than 30 years likely will have lower concentrations due to the high solubility of sulfate. Further sampling would need to be performed to verify this hypothesis.

In general, LK fills also had lower sulfate concentrations. Longer contact time (due to increased time since geologic formation of the geology surrounding LK coal seams) with groundwater could provide a chance for more sulfate to leach out of the geology before the valley fill was constructed. A larger data set with more LK fills older than 12 years would show a more accurate long-term trend.

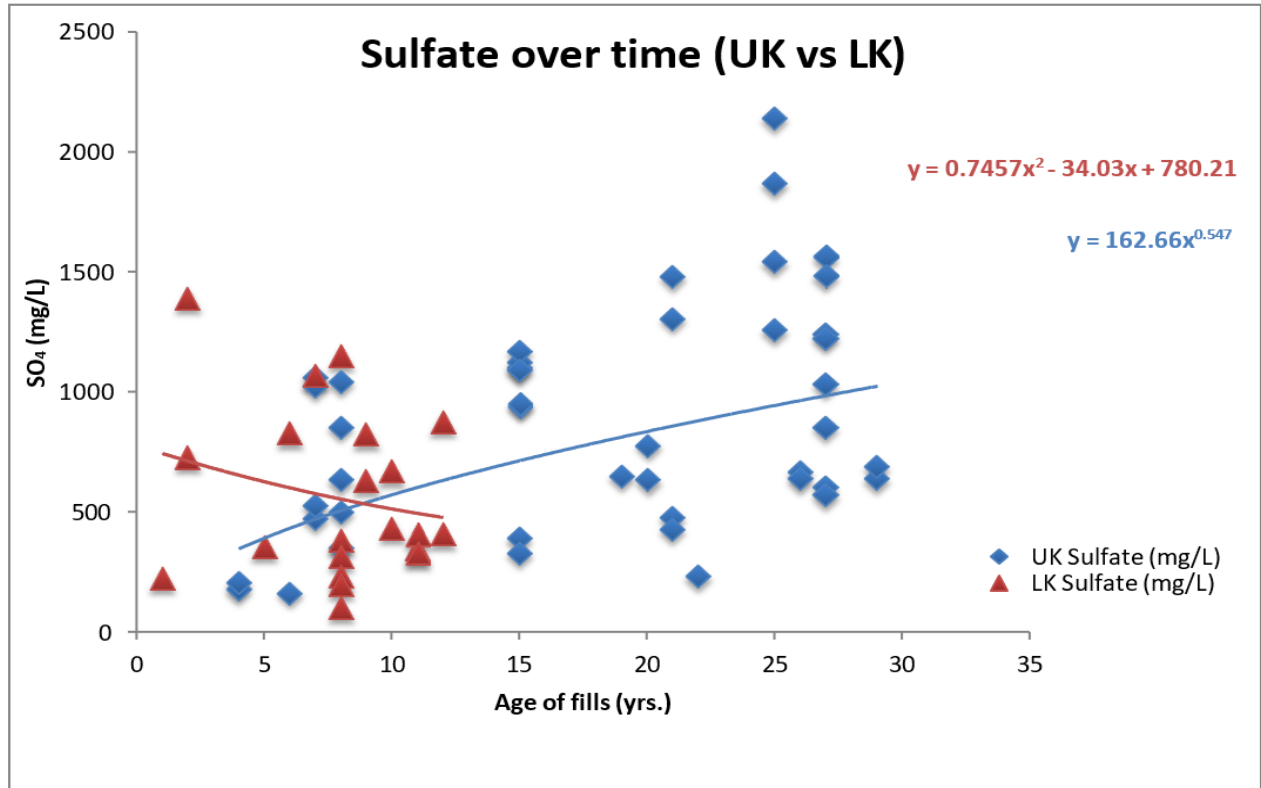


Figure 35: Changes in sulfate concentrations over time as a function of coal seams mined.

### HCO<sub>3</sub>

HCO<sub>3</sub> concentrations showed a similar trend to those of sulfate (**Figure 36**). UK mine concentrations increased slightly over time and LK mines decreased over time. Bicarbonate's low solubility prevents rapid decreases or increases. Correlation between HCO<sub>3</sub> concentrations and fill age were negligible for UK and LK data (**Table 11**).

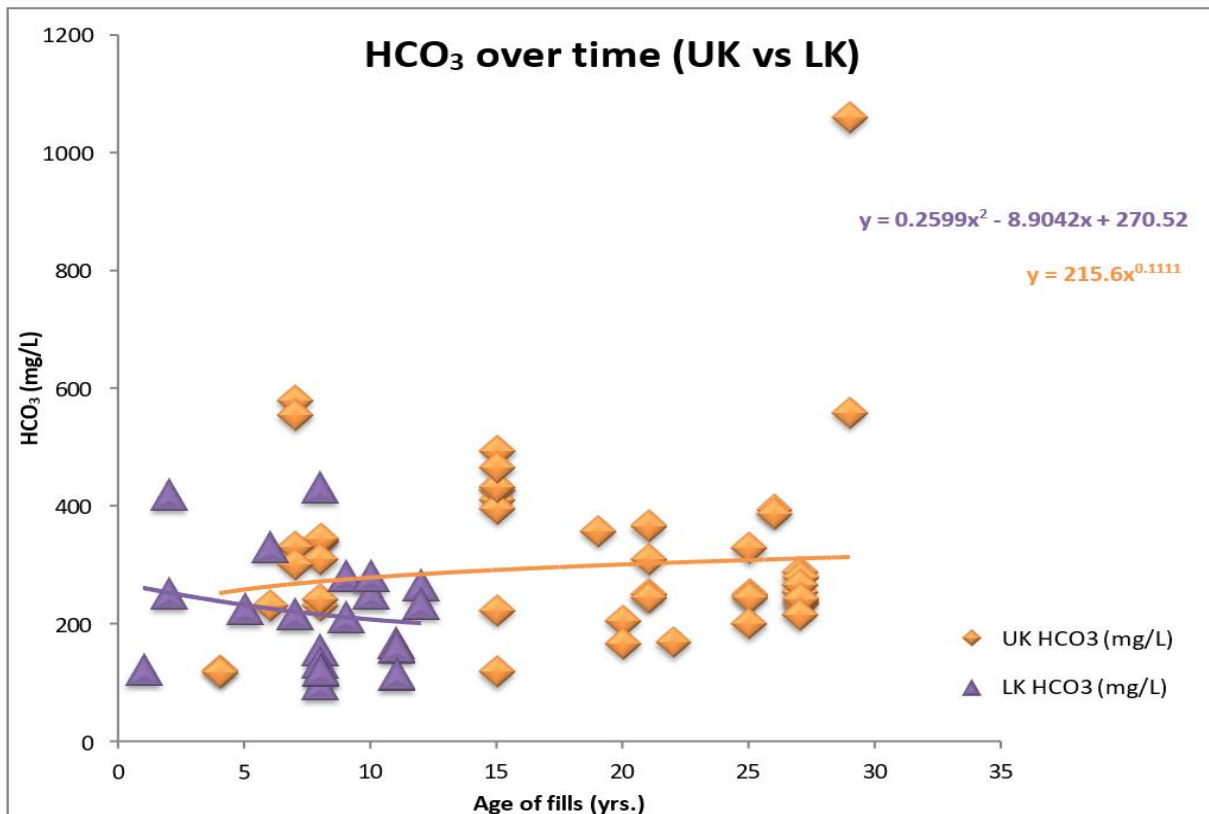


Figure 36: Changes in HCO<sub>3</sub> concentrations over time as a function of coal seams mined.

### Magnesium

Concentrations increased past the age of the oldest fill regardless of valley fill age or coal seams mined (**Figure 37**). A more steady increase was observed in UK coals, indicating continued flushing of magnesium minerals beyond 30 years. The R<sup>2</sup> value for UK mines indicates a moderate correlation between magnesium concentrations and valley fill age. Assuming continuation of the current trend, LK mines would begin to decrease between 15-20 years after fill construction. However, LK mines showed a much lower correlation, indicating that it is unlikely that this trend will continue.

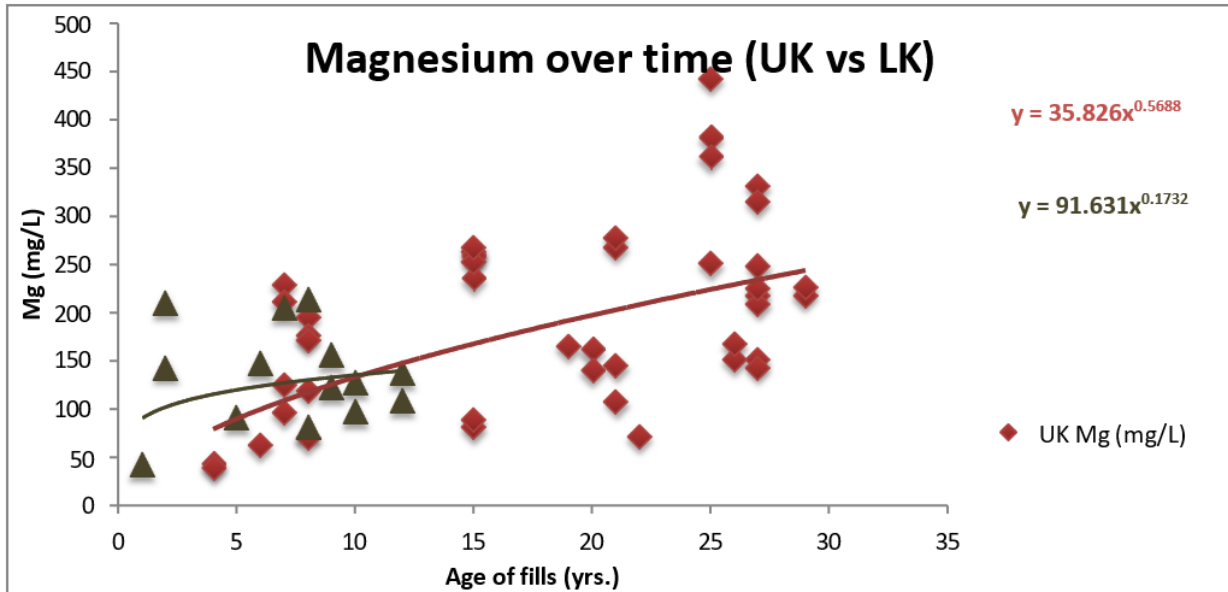


Figure 37: Changes in Mg concentrations over time as a function of coal seams mined.

#### Calcium

Calcium concentrations increased regardless of coal seams mined (**Figure 38**). Rates of increase were very similar, as were  $R^2$  values (**Table 9**). Very low  $R^2$  values indicated negligible correlation between calcium concentrations, fill age, and coal seams mined. More LK mine data from fills greater than 15 years old and UK mine data from fills less than 5 years old would determine if these trends persist.

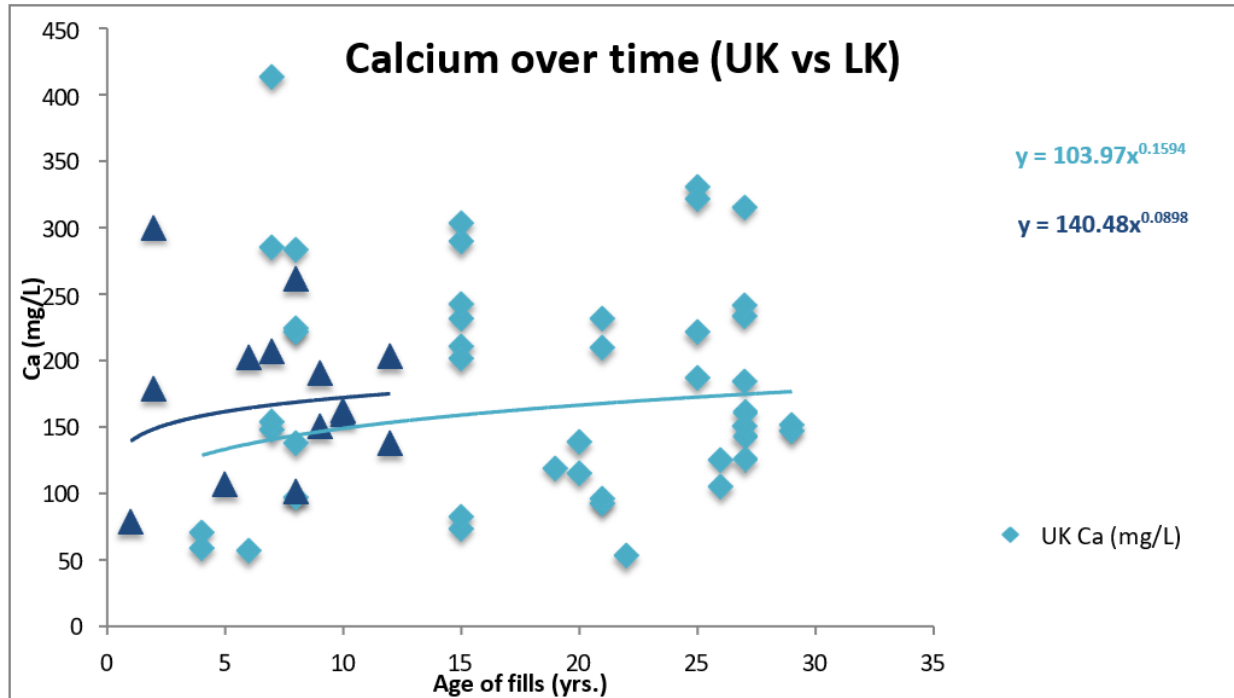


Figure 38: Changes in Ca concentrations over time as a function of coal seams mined.

### Selenium

Selenium had the greatest correlation between fill age and concentrations of all coal seam comparisons (**Table 11**).  $R^2$  values were very similar regardless of coal seams mined. UK mines declined rapidly beginning 7 years after construction and had a 91% reduction after 30 years (**Figure 39**). LK mines decreased by 93%, although lab data for older LK fills was below detectable limits. Leaching rates of approximately this percentage have been determined in other research as well (WRI unpublished data, 2

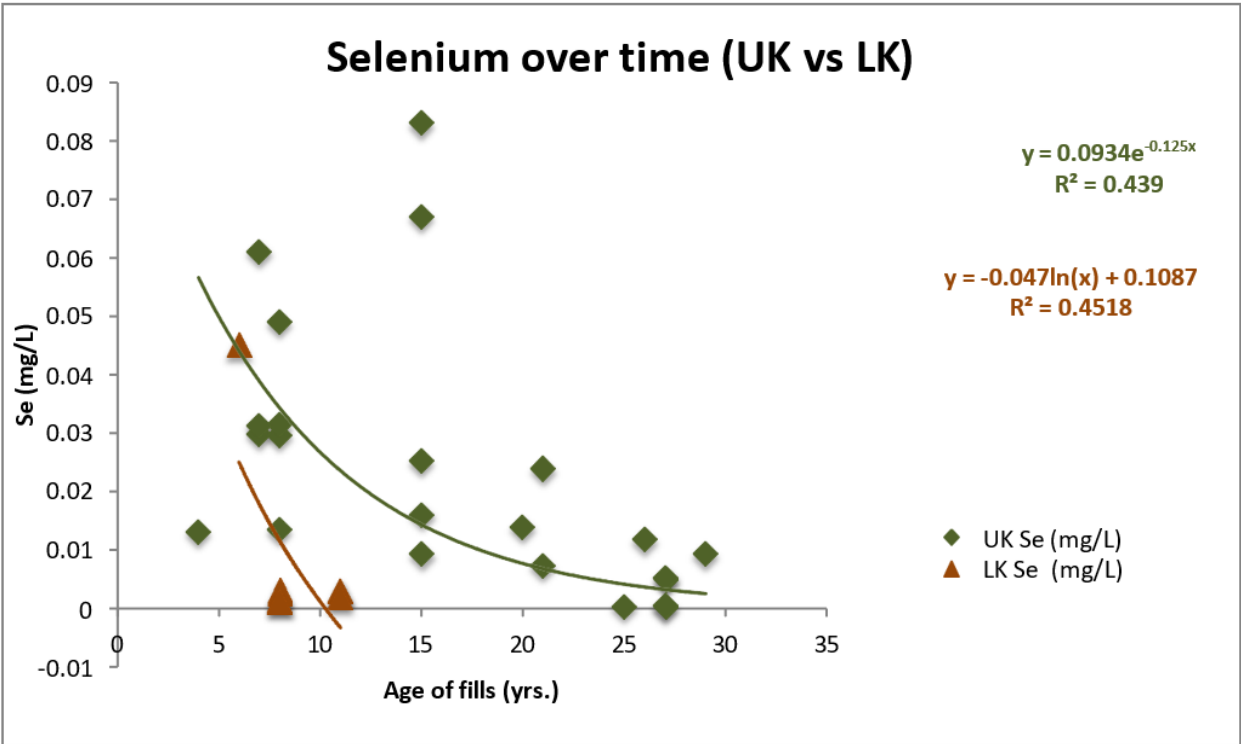


Figure 39: Changes in Se concentrations over time as a function of coal seams mined.

TDS

TDS concentrations from UK mines increased over time. Low R<sup>2</sup> values for both data sets indicate a lack of relationship between TDS, coal seam mined, and valley fill age. On average, UK mines had higher starting TDS concentrations (**Figure 40**). These concentrations continued to increase beyond 30 years after fill construction. TDS concentrations in LK fills decreased over time until fills reached nine years old. From this point, TDS concentrations began to increase. Regardless of coal seam mined, leaching continues to occur within these fills. The rate of leaching appears to be decreasing for UK fills. Many of the more soluble salts likely have already leached from the fill. TDS concentrations should begin to stabilize when only the least soluble salts remain.

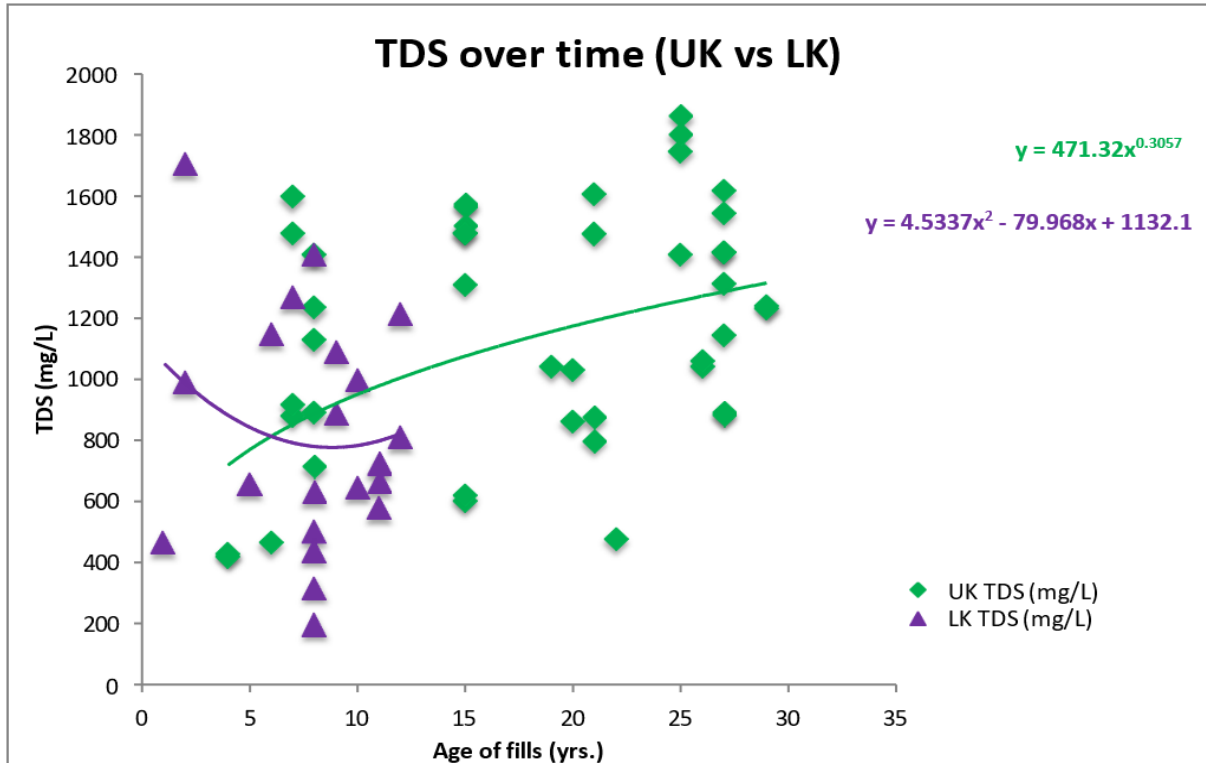


Figure 40: Changes in TDS concentrations over time as a function of coal seams mined.

## Conclusions

Field data, flow values, and water samples were taken from 41 valley fills to determine TDS makeup in southern WV. Data from all fills were used to determine the effects of valley fill age on parameter concentrations. Data were also organized by flow regime and coal seams mined to ascertain the effect of these variables on parameter concentrations.

Sulfate, bicarbonate, calcium, and magnesium made up the largest percentage of TDS. Sulfate, bicarbonate, and magnesium increased for all fills and during high and low flow events. The large concentrations of these ions available within a fill indicate that a longer flushing period may be required before concentrations begin to decrease. A lack of data for fills 0-5 years old could explain concentration increases over time. Calcium showed a slight decrease in concentration over time during high flow. However, concentrations did not begin to decrease until 20 and 18 years after construction for all fills and during low flow, respectively. A combination of low flow and low solubility could explain why the observed decrease did not begin until fills reached at least 18 years old.

Selenium concentrations from all fills and during low flow decreased over time. An observed rapid increase in selenium concentrations during the high flow sample event was likely due to a limited number of data points, as the majority of low flow samples had selenium concentrations below

detectable limits. Selenium concentrations correlated fairly well with valley fill age at both high and low flows ( $R^2$  values of 0.57 and 0.72, respectively).

TDS concentrations increased over time regardless of flow regime. However, TDS concentrations leveled off 19 years after fill construction and began to decrease 21 years after construction during the low flow sampling event. Leaching appears to be continuing within these fills, likely due to continued exposure of previously unweathered material to oxygen and water.

Parameter concentrations were also compared against coal seams mined. Concentrations from UK mines increased over time for sulfate,  $\text{HCO}_3^-$ , and TDS, and these same parameters decreased over time for LK mines. Magnesium and calcium increased over time regardless of coal seam mined. Calcium concentration increases were nearly identical regardless of coal seam mined.

Selenium had the greatest correlation between fill age and concentrations of all coal seam comparisons. UK mines declined rapidly beginning 7 years after construction and had a 91% reduction after 30 years and LK mines decreased by 93%. Leaching rates of approximately this percentage have been determined in other research as well.

One limitation in the current data set is a lack of sampling data involving valley fills between the ages of 0-5 years. With the exception of selenium, the low  $R^2$  values found in the current data do not indicate that a noteworthy correlation between valley fill age and parameter concentration exists. However, the results of this study are a prelude to future research. Subsequent research will include studying the potential impacts from other factors such as valley fill volume/size and upstream watershed area, as well as further study of parameters researched in the current study effort including discharge and geology. Increasing the size of the study area also may show that the data trends found from these fills are vastly different than other fills.

These curves are the best model fit for the current sampling. However, the trends may change with continued sampling. We expect many of the studied parameters to decrease over time. The rate of the expected decrease will be dependent upon multiple factors, including solubility and initial concentration of the parameter.

## References

- Demchak, J. 2005. Water quality changes of underground mines in northern West Virginia. PhD dissertation. West Virginia University, 2005.
- Jones, P.M., Mulvay, S.M., and Fish, D. 1994. The role of sulfate and ionic strength on the shift from acid to alkaline mine drainage in southwest Pennsylvania. pp. 289-295 *In*: Proceedings of the International Land Reclamation and Mine Drainage Conference and the Third International Conference of the Abatement of Acid Mine Drainage. Vol. 2: Mine Drainage. US Bureau of Mines Special Publication SP 06B-94.

- Mack, B., L. M. McDonald and J. Skousen. 2010. Acidity Decay of Above-Drainage Underground Mines in West Virginia. *J. Environ. Qual.* 39:1–8 (2010).
- Meek, F.A. 1996. Evaluation of acid prevention techniques used in surface mining. Chapt.11. *In: Acid Mine Drainage Control and Treatment.* National Mine Land Reclamation Center, Morgantown, WV.
- Mullenex, R.H. 2005. Stratigraphic distribution of selenium in upper Kanawha-lower Allegheny formation strata at a location in southern West Virginia. Poster, 23<sup>rd</sup> annual International Pittsburgh Coal Conf. Pittsburgh, PA.
- Roy, M. 2005. A detailed sequential extraction study of selenium in coal and coal-associated strata from a coal mine in West Virginia. MS thesis, Dept. of Geology and Geography, West Virginia University, Morgantown, WV.
- Vesper, D.J., Bryant, G., and Ziemkiewicz, P.F. 2004. A preliminary study on the speciation of selenium in a West Virginia watershed *In Proceedings of 21<sup>st</sup> annual meeting of the American Society of Mining and Reclamation.* Morgantown, WV. p.1950-1959.
- Wood, S.C., P.L. Younger, and N.S. Robins. 1999. Long-term changes in the quality of polluted minewater discharges from abandoned underground coal workings in Scotland. *Quarterly J. Engineering Geology* 32: 69-79.
- WVWRI. 2010. Unpublished data.
- Younger, P.L. 1997. The longevity of minewater pollution: a basis for decision-making. *The Science of the Total Environment.* 194-195: 457-466.
- Ziemkiewicz, P.F., O'Neal, M., and Lovett, R.J. 2011. Selenium leaching kinetics and in-situ control. *Mine Water Environ* 30: 141-150.